

2015

Physicochemical gradients, diffusive flux and biostabilization of oil sands tailings material

Thomas Reid
University of Windsor

Follow this and additional works at: <http://scholar.uwindsor.ca/etd>

Recommended Citation

Reid, Thomas, "Physicochemical gradients, diffusive flux and biostabilization of oil sands tailings material" (2015). *Electronic Theses and Dissertations*. Paper 5683.

This online database contains the full-text of PhD dissertations and Masters' theses of University of Windsor students from 1954 forward. These documents are made available for personal study and research purposes only, in accordance with the Canadian Copyright Act and the Creative Commons license—CC BY-NC-ND (Attribution, Non-Commercial, No Derivative Works). Under this license, works must always be attributed to the copyright holder (original author), cannot be used for any commercial purposes, and may not be altered. Any other use would require the permission of the copyright holder. Students may inquire about withdrawing their dissertation and/or thesis from this database. For additional inquiries, please contact the repository administrator via email (scholarship@uwindsor.ca) or by telephone at 519-253-3000ext. 3208.

**PHYSICOCHEMICAL GRADIENTS, DIFFUSIVE FLUX AND BIOSTABILIZATION OF
OIL SANDS TAILINGS MATERIAL**

By

Thomas C. Reid

A Thesis
Submitted to the Faculty of Graduate Studies
Through the Great Lakes Institute for Environmental Research
In partial fulfillment of the requirements for
The Degree of Master of Science
At the University of Windsor

Windsor, Ontario, Canada

2014

© 2014 Thomas C. Reid

**PHYSICOCHEMICAL GRADIENTS, DIFFUSIVE FLUX AND BIOSTABILIZATION OF
OIL SANDS TAILINGS MATERIAL**

By

Thomas C. Reid

APPROVED BY:

Dr. D. Haffner

Great Lakes Institute for Environmental Research

Dr. I. Droppo

Environment Canada, National Water Research Institute

Dr. C. Weisener, Advisor

Great Lakes Institute for Environmental Research

January 21, 2015

DECLARATION OF CO-AUTHORSHIP AND PREVIOUS PUBLICATION

I. Co-Authorship Declaration

I hereby declare that this thesis incorporates material that is result of joint research, as follows:

This thesis incorporates the outcome of joint research undertaken in collaboration with R. Boudens, D. VanMensel, S. Prakasan M.R., and J. Ciborowski under the supervision of C. Weisener. This collaboration is covered in Chapter 2 of this thesis. In all cases, primary contributions, experimental designs, data analysis and interpretation were performed by the author, and the contribution of the co-authors was primarily through the provision of instrumentation, laboratory assistance, experimental guidance and manuscript commentary.

This thesis also incorporates the outcome of joint research undertaken in collaboration with I. Droppo under the supervision of C. Weisener. This collaboration is covered in Chapter 3 of this thesis. In all cases, the key ideas, primary contributions, experimental designs, data analysis and interpretation were performed by the author, and the contribution of the co-author was primarily through the provision of instrumentation, laboratory assistance, experimental guidance and manuscript commentary.

I am aware of the University of Windsor Senate Policy on Authorship and I certify that I have properly acknowledged the contribution of the other researchers to my thesis, and have obtained written permission from the co-author to include the above material in my thesis.

I certify that, with the above qualification, this thesis, and the research to which it refers, is the product of my own work.

II. Declaration of Previous Publication

This thesis includes 2 original papers that will be submitted for publication in peer-reviewed journals, as follows:

Thesis Chapter	Publication title/full citation	Publication Status
Chapter 2	Reid, T., Boudens, R., VanMensel, D., Sabari Prakasan, M.R., Ciborowski, J.J.H., Weisener, C.G. 2015. Physicochemical gradients, diffusive flux, and sediment oxygen demand within oil sands tailings materials from Alberta, Canada	<i>Submitted to Applied Geochemistry</i>
Chapter 3	Reid, T., Droppo, I., Weisener, C.G. 2015 Critical shear strength and biostabilization effects of industrial tailings material	<i>In preparation</i>

I certify that I have obtained a written permission from the copyright owner(s) to include the above-published materials(s) in my thesis. I certify that the above material describes work completed during my registration as a graduate student at the University of Windsor.

I declare that, to the best of my knowledge, my thesis does not infringe upon anyone's copyright nor violate any proprietary rights and that any ideas, techniques, quotations, or any other material from the work of other people included in my thesis, published or otherwise, are fully acknowledged in accordance with the standard referencing practices. Furthermore, to the extent that I have included copyrighted material that surpasses the bounds of fair dealing within the meaning of the Canada Copyright Act, I certify that I have obtained a written permission from the copyright owners(s) to include such material(s) in my thesis.

I declare that this is a true copy of my thesis, including any final revisions, as approved by my thesis committee and the Graduate Studies office, and that this thesis has not been submitted for a higher degree to any other University or Institution.

ABSTRACT

Extraction of raw bitumen from the Athabasca Oil Sands through open-pit mining produces waste materials called tailings, which are housed in large settling basins called tailings ponds. As consolidation of fines (sands, silts and clays) occurs, biogeochemical cycling of nutrients and an overall REDOX environment establishes, as with any natural wetland or lake sediment environment. These biogeochemical processes play a role in the dynamic nature of these tailings ponds over time, and directly implicate the future fate of these ponds as they are prepared for reclamation to wetlands or End-Pit Lake environments. This thesis tracks general chemistry and physico-chemical gradients within two different tailings materials over the course of the study, providing measurements of O_2 and HS^- diffusive flux measurements at the tailings-water interface. Further, the effects of biota on the stabilization of these tailings materials, when subjected to an applied shear stress at the interface is studied, with implications on sediment/contaminant erosion and transport.

ACKNOWLEDGEMENTS

I would like to thank my supervisor Dr. Chris Weisener and Dr. Ian Droppo for their help and support during my research. I would also like to thank Dr. Doug Haffner for his insight and thoughts as one of my committee members. Thank you to Dr. Robert Pasuta for his logistical help and use of laboratory space in the sterilization of my (many) samples, as well as Bill Middleton for the use of his instrumentation and guidance with gas chromatography techniques. Many thanks to Mary Lou Scratch and Vera Barker for their administrative assistance with all the paperwork and material needed to complete my degree. Thanks to Dr. Rao Chaganti who was always available to help with troubleshooting or simply discussing ideas related to DNA/RNA isolation and preservation. Thank you to my GLIER friends and lab mates, particularly Nadine Loick and Rachel Franzblau who helped get me situated in the lab, as well as Ryan Boudens, Danielle VanMensel, Sabari Prakasan M.R., Zach Diloretto and Nick Falk who always lent a helping hand. Finally, I would like to give a big thanks to my wife for her unending support, my daughter Wynne, and of my family and friends who have always supported and guided me in whatever I have done.

TABLE OF CONTENTS

DECLARATION OF CO-AUTHORSHIP AND PREVIOUS PUBLICATION	iii
ABSTRACT	v
ACKNOWLEDGEMENTS	vi
LIST OF TABLES	x
LIST OF FIGURES	xi
CHAPTER 1: INTRODUCTION	
<i>1.1. Athabasca Oil Sands</i>	1
<i>1.2. Biogeochemistry of Tailings Ponds</i>	2
<i>1.3. Sediment Shear Strength and Biostabilization of Tailings</i>	8
<i>1.4. Research Scope</i>	9
<i>1.5. Hypotheses</i>	12
<i>1.6. Objectives & Predictions</i>	14
<i>1.7. References</i>	19
CHAPTER 2: PHYSICOCHEMICAL GRADIENTS, DIFFUSIVE FLUX, AND SEDIMENT OXYGEN DEMAND WITHIN OIL SANDS TAILINGS MATERIAL FROM ALBERTA, CANADA	
<i>2.1 Introduction</i>	23
<i>2.2 Methods</i>	24
<i>2.2.1 Laboratory Microcosms</i>	24
<i>2.2.2 Microsensor chemical profiles</i>	26

2.2.3 Diffusivity Calculations & Chemical Flux	27
2.2.4 Gas Expression	28
2.3 Results and Discussion	
2.3.1 Biogeochemical alteration of FFT materials	28
2.3.2 Dissolved Oxygen	30
2.3.3 HS ⁻ Production	32
2.3.4 Oxygen & Hydrogen Sulfide Diffusivity and Flux	
2.3.4.1 App. Diffusivity measurements for P1A and STP	33
2.3.4.2 Dissolved Oxygen Flux	34
2.3.4.3 Hydrogen Sulfide Flux	36
2.3.5 Headspace methane expression	38
2.4 Conclusions	41
2.5 References	49

CHAPTER 3: CRITICAL SHEAR STRENGTH AND BIOSTABILIZATION EFFECTS ON INDUSTRIAL TAILINGS MATERIAL

3.1 Introduction	53
3.2 Methods	
3.2.1 Experimental design – GUST microcosm	55
3.2.2 FFT Microcosm/Core set-up	56
3.2.3 Experimental Procedure	
3.2.3.1 GUST Chamber	57
3.2.3.2 DNA expression	58

<i>3.3 Results and Discussion</i>	
<i>3.3.1 GUST microcosm shear strength</i>	59
<i>3.3.2 Cumulative Eroded Mass</i>	63
<i>3.3.3 Microbial Community Structure</i>	64
<i>3.4 Conclusions</i>	66
<i>3.5 Future Work and Improvements</i>	68
<i>3.6 References</i>	85
 CHAPTER 4: CONCLUSIONS, LIMITATIONS AND FUTURE DIRECTION	
<i>4.1 Summary and Conclusions</i>	88
<i>4.2 Limitations and Future Work</i>	90
<i>4.3 References</i>	92
 Appendix A	93
 VITA AUCTORIS	98

LIST OF TABLES

CHAPTER 2:

TABLE 2.1: Experimental design comparing 2 tailings	48
TABLE 2.2: Description of bulk FFT material	49
TABLE 2.3: Apparent Diffusivity measurements	50
TABLE 2.4: DO flux measurements	51
TABLE 2.5: DO flux comparison to natural systems	52
TABLE 2.6: HS ⁻ flux measurements	53
TABLE 2.7: HS ⁻ flux comparison to natural systems	54

CHAPTER 3:

TABLE 3.1: Microcosm/Core set-up for U-GEMS system	90
TABLE 3.2: Experimental applied shear stresses on FFT	91
TABLE 3.3: Comparison of critical shear strength measurements	92

LIST OF FIGURES

CHAPTER 1:

FIGURE 1.1: Map of the Athabasca Oil Sands region	17
FIGURE 1.2: Oil sands tailings pond schematic	18
FIGURE 1.3: Suncor Mining Operation	18

CHAPTER 2:

FIGURE 2.1: Microsensors attached to micromanipulator	44
FIGURE 2.2: Visible physical alteration of FFT	45
FIGURE 2.3: Example of rapid initial consolidation	46
FIGURE 2.4: Headspace methane concentrations	47

CHAPTER 3:

FIGURE 3.1: Experimental Design of U-GEMS System	75
FIGURE 3.2: Shear strength experimental set-up	76
FIGURE 3.3: GUST microcosm with 10cm water column	77
FIGURE 3.4: Turbidity vs. Shear stress plot for biotic Pond STP (Erosion#1)	78
FIGURE 3.5: Turbidity vs. Shear stress plot for abiotic Pond STP (Erosion#1)	79
FIGURE 3.6: Turbidity vs. Shear stress plot for biotic Pond 1A (Erosion#1)	80
FIGURE 3.7: Turbidity vs. Shear stress plot for abiotic Pond 1A (Erosion#1)	81
FIGURE 3.8: Turbidity vs. Shear stress plot for biotic Pond STP (Erosion#2)	82
FIGURE 3.9: Turbidity vs. Shear stress plot for abiotic Pond STP (Erosion#2)	83
FIGURE 3.10: Turbidity vs. Shear stress plot for biotic Pond 1A (Erosion#2)	84

FIGURE 3.11: Turbidity vs. Shear stress plot for biotic Pond 1A (Erosion#2)	85
FIGURE 3.12: Comparison of the cumulative eroded mass by shear stress	
Pond 1A	86
FIGURE 3.13: Comparison of the cumulative eroded mass by shear stress	
Pond STP	87
FIGURE 3.14: Microbial community hierarchy by phylum	88
FIGURE 3.15: Classes of <i>Proteobacteria</i> in Pond 1A and Pond STP	89

CHAPTER 1

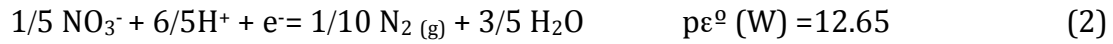
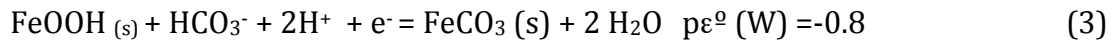
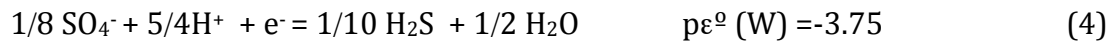
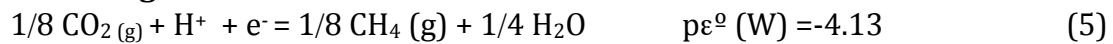
INTRODUCTION

1.1. Athabasca Oil Sands

Producing approximately 1.9 million barrels of bitumen a day, the Athabasca oil sands in Alberta, Canada (Figure 1.1) continues to increase production rates as the conventional oil reservoirs decline globally and more efficient, less costly extraction techniques are developed (Alberta Energy, 2013; Williams, 2003; CAPP, 2014). During open-pit mining of bitumen, separation of the bitumen from raw ore through hot water extraction, results in large amounts of waste material known as tailings (CAPP, 2014). These initial tailings consist of 55 wt.% solids (silts, clays and sands), and contain ~1% residual bitumen, and alkaline processed waters (Chalaturnyk et al. 2002), which are pumped into large settling basins known as tailings ponds, where the solids are allowed to settle out, forming semi-consolidated fluid fine tailings (FFT). Compliance with a zero-discharge policy is mandatory, requiring oil companies to provide suitable containment for oil sands processed materials (OSPM). The basins themselves allow for the recycling of process waters to reduce consumption of fresh water sources (Alberta Energy, 2013). Part of the rehabilitation plan involves two possible options 1) conversion to natural wetlands or 2) the development of End-Pit Lake (EPLs) ecosystems. Given the scale of these tailings environments, it is vital to understand the chemical and biological processes at the FFT-water interface, and how these interactions dictate or influence the long-term fate of such EPLs or remediated wetland environments.

1.2. Biogeochemistry of Tailings Ponds

The geochemical gradients and corresponding chemical diffusive fluxes within the FFT, as with any aquatic or marine sediment, can change significantly during the consolidation process, and are affected by the very material comprising the FFT as well as the complex microbial consortia within each individual pond (Fedorak et al., 2002; Penner and Foght, 2010; Chi Fru et al. 2013). Further this biogeochemical activity within the FFT has direct impact on the quality and composition of the cap water. Depletion of dissolved oxygen (DO), along with other nutrient cycles such as iron cycling, denitrification and the production of both hydrogen sulfide (H_2S or HS^-) and methane (CH_4) are indicators of reducing conditions that can directly or indirectly influence aquatic organisms inhabiting these environments. These chemically reducing processes are commonly observed not only in water logged tailings materials, but also can be observed in natural marine and wetland settings where organic matter is prone to degradation, and other terminal electron acceptors will dominate in the absence of O_2 (Froelich et al., 1979). An illustration of this is shown in equations 1-5, which show the succession of reduction pathways in order from most to least favorable energy yield (Stumm and Morgan, 1995). Only once O_2 is fully depleted will denitrification begin, and once this process has depleted the nitrogen pool, iron reduction takes hold and so on.

Aerobic Respiration**Denitrification****Iron Reduction****Sulfate Reduction****Methanogenesis**

However, as is often the case in real world scenarios, this textbook understanding of the thermodynamic REDOX ladder fails to stand true in many study systems, indicated by Bethke et al., 2011. In this study, there was no fixed thermodynamic hierarchy between iron reducers, sulfate reducers (SRBs) and methanogens. Natural systems, for example, may allow for sulfate reducers to be active alongside iron reducing processes (Bethke et al., 2008), indicating microbial activity is not governed by usable energy levels alone. In addition, the prescribed competition for electron donors was not observed in that study. Instead a co-operative existence was observed, where, for example, Fe^{2+} and HS^- was produced in a one-to-one relation forming precipitated FeS minerals (Bethke, et al., 2011). This observation is also observed in Ramos-Padron et al. (2011), where large concentrations of dissolved H_2S reacts with iron in oil sands tailings material, forming extensive FeS mineralization, trapping a large proportion of sulfides within the tailings. Finally, Bethke et al. (2011) also observed that methanogens and sulfate

reducers have nearly indistinguishable usable energy levels in natural groundwater systems, further disputing the notion of thermodynamically favored REDOX ladder. Overall, this interrelated series of chemical reactions play a dominant role in the evolution of these tailings ponds, and inevitably dictate the fate of EPLs and remediated wetlands in the future. Such reactions therefore directly affect DO concentrations within the water column due to oxidation pathways possible with these reduced N_2 , Fe, and H_2S compounds. Perhaps the most dominant of these processes include the cycling of Fe and SO_4 , which form visible and distinct REDOX zones in the upper-most fluid fine tailings layers as observed in several studies (Stasik et al. 2014, Chen et al. 2013).

However, in addition to the cycling of Fe and S within these systems, methanogenesis also plays a significant role in the carbon degradation processes, and is perhaps more complex in nature. It is the end process of the microbial metabolism of organic matter (assuming a thermodynamic hierarchy of redox processes), and has become a concern due to increasing greenhouse gas (GHG) emissions. As all other electron acceptors become depleted (O_2 , NO_3 , Fe, SO_4), the remaining carbon source (CO_2) as well as H_2 and residual organics are used in the microbial production of CH_4 . There have been multiple studies on the production of methane from various wetland and marine environments, landfills and even similar tailings ponds to those described in this thesis, given its significance to the overall GHG proportions. Further, within these oil sands tailings ponds, several studies have given insight into the competition between sulfate reducing bacteria and methanogens, since both are competing for the same electron donors (Holowenko et

al., 2000; Fedorak et al., 2002). Though, as described earlier, perhaps this *competition* for electron donors is more of a delicate balance between the sulfate reducers and methanogens (Bethke et al., 2011), thus increasing our need for a holistic understanding of these systems from a holistic biogeochemical framework.

Sediment oxygen demand (SOD) is an indicator used to evaluate the baseline response of tailings materials for use in reclaimed wetlands or EPLs. The term applies to both biological oxygen demand (BOD) and chemical oxygen demand (COD) processes dominating sediments, and represents the consumption of DO by the various chemically driven processes and decay of organic matter at the water-sediment boundary via respiration by aerobic organisms (APHA. 1992). This consumption of oxygen at the sediment-water interface can exceed the downward flux of atmospheric O₂ within the water column leading to hypoxia. It is generally accepted that DO levels below ~2 mg L⁻¹ are too low to sustain most fish species, and at levels below even ~6 mg L⁻¹ some cold water fish species (i.e. Salmon, trout etc.) are unable to reproduce (Carter, 2005).

Chen et al. in 2013 investigated the DO behavior and sulfur cycling associated with FFT collected from West-In Pit Lake (WIP) storage basin operated by Syncrude Canada Ltd. The study identified an aforementioned sulfidic zone within biotic systems, providing insight into the microbial role in the cycling of S within the FFT materials. Further, in oxic systems, O₂ consumption was enhanced in the biotic systems compared to the abiotic controls, due in part to the biota forming reduced reactants over time. However, both abiotic and biotic treatments reported negligible O₂ within the FFT at the onset of the experiment, suggesting that both

biologically and chemically driven processes contribute to overall SOD, though the DO gradient of the biotic system indicated increased consumption, thus $BOD > COD$ (Chen et al. 2013). Hydrogen sulfide production correlated strongly with the biotic systems, with HS^- concentrations in the FFT reaching $86 \mu\text{mol L}^{-1}$ after 5 weeks, while the abiotic systems remained at a background of $<10 \mu\text{mol L}^{-1}$ throughout their study (Chen et al. 2013).

The diffusive chemical flux is a term used to describe the mobility of molecules within a certain substance, transporting from an area of high concentration to low concentration, directly correlating to the steepness of a measured concentration gradient. Diffusive flux measurements across water-sediment boundaries and has been studied extensively over several decades (Boudreau and Guinasso 1982; Jørgensen and Revsbech 1985; Jørgensen and Marais 1990; Lorke et al. 2003). The so-called diffusive boundary layer (DBL), or benthic boundary layer (BBL) creates distinct concentration gradients, and has direct impact on the overlying water column (Brand et al. 2007). In this thin layer above the sediment, the dominant transport mechanism is molecular diffusion (Gundersen and Jørgensen 1990), therefore, it is highly advantageous to determine diffusive flux values across this interface in accordance with both O_2 and HS^- concentrations. Diffusive flux across the DBL directly relates to the physical properties of the FFT, and can correlate directly to the diffusive properties within its mineralogical matrix. Furthermore, biofilm structure, be it thin and porous or tightknit and thick affect the diffusive characteristics of various molecules across the DBL (Tijhuis et al., 1994).

This study compares the biogeochemical development of FFT materials collected from two different tailing pond sources Pond STP and Pond 1A from Suncor Energy Inc. Pond 1A is a inactive water recycling pond containing aged FFT approximately 38 years old while STP pond is an active tailings pond still in operation which receives fresh mixed tailings on an ongoing basis. This study will investigate the behavior of DO and S across the DBL associated with two different FFT materials using a series of microcosms after Chen et al. 2013. In this investigation, distinct biogeochemical gradients were observed based on FFT type, and provide further insight into the processes being regulated by biotic and abiotic activity influencing oxygen and sulfur dynamics. Tracking the DO concentrations in the water column over the course of this study will give insight into the long-term SOD, and whether or not DO increases or decreases over time. Further, a brief summary of the distinct redox zonation will be presented, explaining influences on the cycling of key elements such as Fe and S species within each respective pond. Specific diffusive flux measurements will be presented in order to gain an understanding of the diffusive nature of the materials with respect to O_2 flux in, and HS^- flux out of the FFT. Finally a brief comparison of methane concentration in microcosm headspaces will be explained, giving insight into the unique nature of these tailings systems. These results will be beneficial for future development of conceptual and numerical models used to predict biogeochemical cycling and SOD within tailings ponds as EPLs and natural wetland environments are developed.

1.3. Sediment Shear Strength and Biostabilization of Tailings Material

When characterizing any sediment either physically or chemically, erodibility is an important consideration because it directly correlates to the transportation of nutrients, metals and other contaminants. Erodibility is the sediments likeliness of being resuspended in the water column, and is caused by hydrodynamic forces such as wave action, tidal forces and biogeochemical activity (e.g. gas bubbling/ebullition). On a micro level, sediment grains will naturally bond by cohesive forces such as water surface tension and atomic forces (Mehta, 1989), while gravity and microbial processes will cause densification of sediment over time. However, once the shear stresses caused by water column hydrodynamics exceeds the cohesive force of the sediment, resuspension and ultimately transportation of sediment will occur (Paterson 1997; Tolhurst et al. 1999). This cohesive threshold of the sediment is referred to as the sediment shear strength, or the sediment's resistance to resuspension and erosion. In recent years, sediment shear strengths have become an ever more intriguing subject due to implications on contaminant transport. One research paper by Wang et al. (2000) studied the effects of storm events on the sediment of an estuary. This study found that tidal cycles resuspended the loosely consolidated materials, while storm events, with their higher bottom stresses, saw resuspension and erosion of more consolidated materials. Another study by Droppo et al. (2001) studied, in situ, the bed stability in Hamilton Harbour, Lake Ontario. This study focused on the structure and stability of the top-most, "fluffy" layer of sediment. It was concluded that this surface layer, referred to as lacustrine surface fine-grained laminae (SFGL), was biostabilized through biofilm structures that

formed a matrix throughout the sediment. This matrix is composed of extracellular polymeric substances (EPS) (Decho, 1990; Donlan, 2002; Flemming, 2011), and has been observed to significantly increase the shear strength of sediments. Further, in earlier studies (Stone and Droppo, 1994; Levesque & De Boer, 2000), it was observed that these SFGL are often associated with high metal concentrations, and act as a short-term sink. Therefore, the resuspension of the SFGL is potentially remobilizing the heavy metals into the water column, which is of obvious concern in certain ecosystems. Another study by Droppo et al. in 2007 went on to examine the effects of varying biofilm stage with sediment stability. This study found that depending on biofilm development stage, sediment shear strength could be increased, followed by periods of lower stabilization. However, it is clear that biotic component in the sediment will always be more stable than abiotic sediments, due to the cohesive properties of biological exudates such as microbial produced EPS, unless there is an alternate means (e.g. heavy consolidation) by which the abiotic system becomes less erodible. Overall, understanding the microbes ability to stabilize these FFT materials will be beneficial to furthering the modeling and predictive tools needed as these tailings ponds are developed into EPLs and reclaimed wetlands. Furthermore, this biostabilization will be a vital characteristic of the FFT as it is transferred into the EPL environments, in that any resistance to disturbance upon mixing will cause rapid settling and flocculation once moved.

1.4. Research Scope

In order for tailings ponds to be reclaimed into End-Pit Lake environments (EPLs) or natural wetlands, an understanding of the complex physical and biogeochemical nature of these systems must be attained prior to development of these reclaimed environments. Chapter 2 explains the first research topic in this thesis, involving a static microcosm study comparing the biogeochemical development of FFT materials collected from two different tailing pond sources Pond STP (STP) and Pond 1A (P1A) from Suncor Energy Inc. (Figure 1.3). P1A is a inactive water recycling pond containing aged FFT approximately 38 years old while STP is an active tailings pond still in operation which receives fresh mixed tailings on an ongoing basis. This study will investigate the behavior of DO and S across the DBL associated with the two different FFT materials using a series of microcosms after Chen et al 2013. In this investigation, distinct biogeochemical gradients were observed based on FFT type, and provide further insight into the processes being regulated by biotic and abiotic activity influencing oxygen and sulfur dynamics. Tracking the DO concentrations in the water column over the course of this study will give insight into the long-term SOD, and whether or not DO increases or decreases over time. Further, a brief summary of the distinct redox zonation will be presented, explaining influences on the cycling of key elements such as Fe and S species within each respective pond. Specific diffusive flux measurements will be presented in order to gain an understanding of the diffusive nature of the materials with respect to O_2 flux in, and HS^- flux out of the FFT. Finally a brief comparison of methane concentration in microcosm headspaces will be proposed, providing

insight into the unique nature of these tailings materials. These results will be beneficial for future development of conceptual and numerical models used to predict biogeochemical cycling and SOD within Alberta's tailings ponds as the industry moves towards development of EPLs and natural wetland environments.

Furthermore, this thesis will provide context for modeling dynamic environments where sediment and/or tailings resuspension can be controlled through water column turbulence (e.g. wave action, temperature, density conversion such as salinity differences etc.). Chapter 3 investigates the physical control on the sediment-water interface disturbed by simulated erosion forces, to determine the shear strength of selected tailings material. Using a novel microcosm system, P1A and STP tailings are compared not only to each other, but also in a biotic vs. abiotic framework. Results on the critical shear strength of the FFT from each pond are discussed, as well as variation between biologically active and sterilized systems and their significance. Specifically, the biotic vs. abiotic experiments are compared to see whether the established indigenous microbial community directly influences the stability of the FFT at the sediment-water interface. Using extracted DNA profiles, comparisons of the microbial community hierarchy at each sediment interface for the Pond 1A and pond STP will be discussed. This collective information can be used to understand FFT consolidation and erosion properties leading to improved management methods to control FFT resuspension.

1.5. Hypotheses

1.5.1. Hypotheses for Static Microcosm Research

Variation in tailings chemistry and native microbial community structure can lead to differences in the evolution of the REDOX state within tailings pond environments. Interactions between the various bacterial communities and available nutrient sources can have direct implication on the cycling of key elements, gas expression and overlying water quality over time. Therefore, research is needed to characterize the tailings pond environments, particularly across the FFT-water interface, in terms of overall chemical and biological contributors to overall SOD. In particular, studies are needed to determine pond-to-pond variability and a comparison to natural wetland or aquatic environments in the future to determine baseline reference site characterization.

Based on the differing characteristics of STP and P1A (e.g. age of ponds and tailings maturity), it is hypothesized that the juvenile STP FFT material will show a delayed onset with respect to the establishment of specific redox qualifiers (e.g. Sulfur and oxygen donors/acceptors) contributing to geophysicochemical gradients observed, compared to the established (aged) P1A FFT material. In part this is due to properties or components within the fresh FFT one of which could be indicative of limited biodiversity (e.g. extremophiles) compared to the aged FFT. Comparing the two systems will allow determination of the biological contributions to and or differences in chemical flux and the microbial drivers as these systems evolve

temporally. In addition to the variation between pond materials, it is also hypothesized that the biotic systems will show distinct biogeochemical alteration, opposed to the abiotic systems lacking any microbial input, therefore acting as a chemically driven representative sample. These hypotheses will be tested in a microcosm-based laboratory study, in which the evolution of two pond materials varying in maturity, will be studied with respect to biotic vs. abiotic drivers.

1.5.2. Hypotheses for Dynamic Shear Strength Research

Laboratory based experiments using constructed static SOD microcosm enclosures have been shown to simulate field conditions with respect to redox character. However, a greater understanding is needed with regards to the behavior of FFT under hydrodynamic stress such as wave action and water turbulence, causing resuspension and erosion, which affects settling patterns of FFT. The effects of biofilms causing enhanced stability in natural systems, has been extensively studied in recent years due to implication of contaminant transport. Quantifying critical shear strengths of various FFT materials will provide greater insight into the interaction of established biofilms with their physical environment. These measured parameters with respect to resuspension and erosion of FFT will further improve models and predictive tools for the development of EPL and natural wetlands.

It is hypothesized that the biofilm present in the biotic tailings material will provide greater stability to the sediment, through the secretion of extracellular

polymeric substances (EPS), and therefore be more resistant to shearing forces caused by wave action and laminar flow. Thus, biotic systems would measure higher critical shear strength, causing erosion at shear stresses higher than those causing resuspension in the abiotic (sterilized) systems. Secondly, the aged P1A FFT will exhibit far higher critical shear strength than the fresh STP FFT, due to considerable consolidation over time. This physical consolidation will inevitably increase the critical shear strength, independent of the cohesive properties of microbial biofilms.

1.6. Objectives and Predictions

1.6.1. Static Microcosm Research

The primary research objectives for the static microcosm research are to compare the evolution of P1A and STP in terms of their physicochemical gradients and diffusive flux measurements across the interface. Further, these diffusive flux measurements will help to determine the overall sediment oxygen demand (SOD), comprised of both the biological (BOD) and chemical (COD) oxygen demands. Furthermore, the expression of methane gas into the headspace will be tracked within the anoxic systems, to characterize the ebullition of CH₄ from the FFT into the overlying water column and headspace. Lastly, general physicochemical alterations are observed and compared between ponds and atmospheric conditions to determine settling/consolidation over time, and FFT coloration changes due to either oxidizing or reducing conditions.

It is predicted that the aged P1A will equilibrate sooner with respect to redox order, than the fresh STP FFT. Further, P1A will likely have a higher flux of HS^- , and will express some quantity of methane in the biotic system, likely attributed to its advanced state of consolidation, therefore more diverse microbial population. STP on the other hand will likely exhibit redox characterization later into the experiment, since it is freshly processed material, perhaps not yet containing a diversified and specialized microbial population. In addition, the liquid nature of the initial STP FFT will inevitably mean that there will be a significant amount of settling over the course of the experiment.

The objectives for the dynamic microcosm experiments are to determine a critical shear strength value for each pond FFT, and for each of the biotic and abiotic treatments. In addition, the overall characterization of the biofilm, in terms of its ability to stabilize the FFT will be studied, in comparison to the natural settling effects of the abiotic system. Finally, subsampling during erosion experiments will be used to determine the microbial community structure within each pond, identifying similarities and differences between them. Any variation in observed microbial consortia can lead to differences in observed FFT shear strength, due to differences in biofilm matrix.

In the dynamic shear strength study, it is predicted, based on studies of natural systems, that the presence of a biofilm will increase the critical shear strength of the FFT, thus resisting forces causing resuspension. Further, the aged

nature of P1A, in which extensive settling and consolidation has already occurred, will inevitably create strengthened bonds between particles, therefore having higher shear strength than STP FFT, which is freshly processed and not consolidated. Finally, the molecular work will likely determine the complexity and diversity of the P1A microbial community, again attributed to its age. The community has had time to diversify and take hold within P1A unlike STP.

Figure 1.1: Map of the Athabasca Oil Sands region, from the Alberta Geological Survey (www.ags.gov.ab.ca)

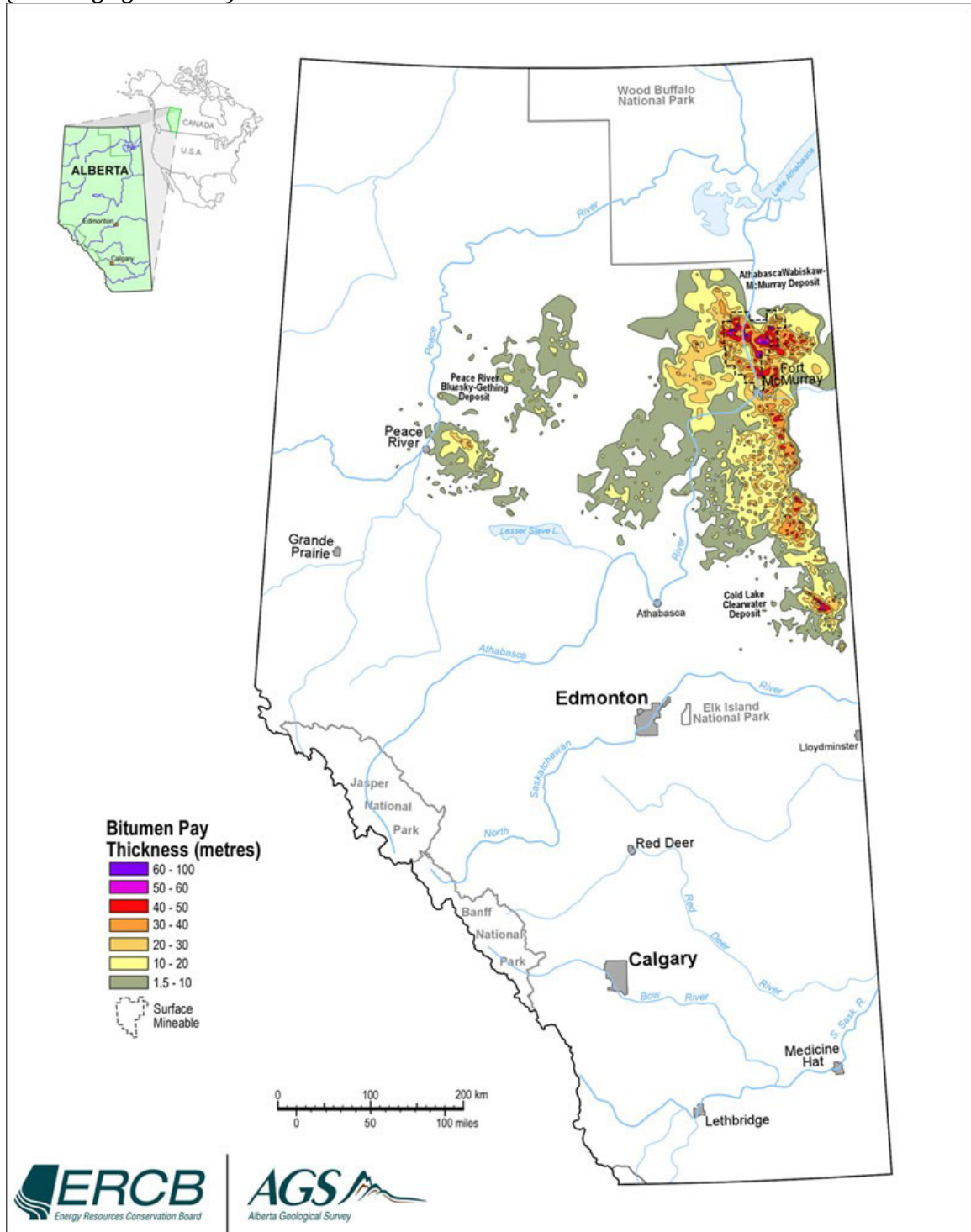


Figure 1.2: Oil sands tailings pond schematic showing containment basin, fluid fine tailings, and recyclable cap water (oilsandstoday.ca)

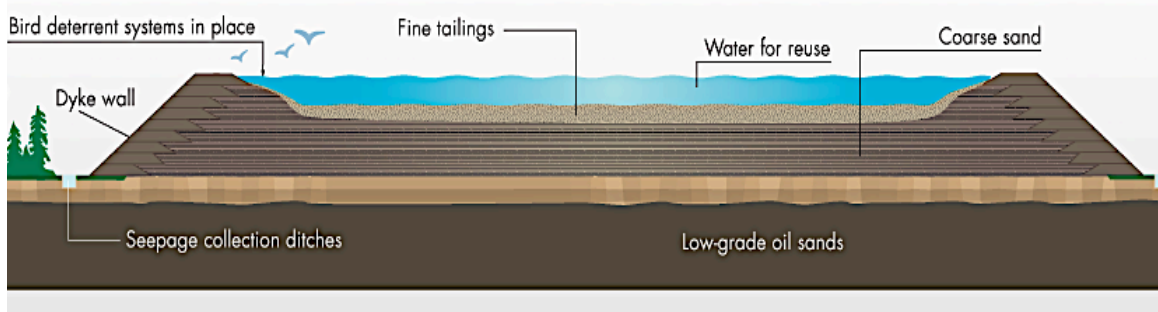


Figure 1.3. Suncor mining operation, showing both Pond 1A (top left) and South Tailings Pond (STP) (bottom right). (taken from Google Maps)



1.7. References

- Alberta Energy Government, 2013. <<http://www.energy.gov.ab.ca/Oil/pdfs/FSRefining.pdf>>.
- APHA. 1992. *Standard methods for the examination of water and wastewater*. 18th ed. American Public Health Association, Washington, DC.
- Bethke, C. M., Ding, D., Jin, Q. S., and Sanford, R. A. 2008. Origin of microbiological zoning in groundwater flows. *Geology*, 36, 739 –742.
- Bethke, C.M., Sanford, R.A., Kirk, M.F., Jin, Q., Flynn. 2011. The thermodynamic ladder in geomicrobiology. *American Journal of Science*. 311:183-210.
- Boudreau, B.P., Guinasso, N.L., 1982. The influence of a dissuasive sublayer on accretion, dissolution, and diagenesis at the sea floor. *In* K.A. Fanning and F.T. Manheim [eds.], *The dynamic environment of the ocean floor*. Lexington.
- Brand, A., Muller, B., Wuest, A., Dinkel, C., Revsbech, N.P., Nielsen, L.P., Pedersen O., Damgaard, L.R., Larsen, L.H., Wehrli, B. 2007. Microsensor for in situ flow measurements in benthic boundary layers at submillimeter resolution with extremely slow flow. *Limnol. And Oceanogr.: Meth.*, 5, 185 – 191.
- Carter, K. (2005, August). The Effects of Dissolved Oxygen on Steelhead Trout, Coho Salmon, and Chinook Salmon Biology and Function by Life Stage . In California Regional Water Quality Control Board, North Coast Region. Retrieved from http://www.swrcb.ca.gov/northcoast/water_issues/programs/tmdls/shasta_river/060707/29appendixbethetheeffectsofdissolvedoxygenonsteelheadtroutcohosalmonandchinooksalmonbiologyandfunction.pdf
- Chalaturnyk, R.J., Scott, J.D., .züm, B., 2002. Management of oil sands tailings. *Petrol. Sci. Technol.* 20, 1025–1046.
- Chen, M., Walshe, G., Chi Fru, E., Ciborowski, J.H., Weisener, C.G. 2013. Microcosm assessment of the biogeochemical development of sulfur and oxygen in oil sands fluid fine tailings. *App. Geochem.*, 37, 1 – 11.

- Chi Fru, E., Chen, M., Walshe, G., Penner, T., Weisener, C.G. 2013. Bioreactor studies predict whole microbial population dynamics in oil sands tailings ponds. *Applied Microb. and Biotechnol.*, 97(7), 3215 – 3224.
- Crude Oil: Forecast, Markets and Transportation. June 2014. Canadian Association of Petroleum Producers. www.capp.ca
- Decho A.W., 1990. Microbial exopolymer secretions in ocean environments – their role(s) in food webs and marine processes. *Oceanography and Marine Biology*, 28, 73–153.
- Donlan, R.M. 2002. Biofilms: microbial life on surfaces. *Emerging Infectious Diseases* 8, 881–890.
- Droppo, I.G., Amos, C.L., 2001. Structure, stability and transformation of contaminated lacustrine surface fine-grained laminae. *J. Sediment. Res.* 71, 717 - 726.
- Droppo, I.G., Ross, N., Skafel, M., Liss, S.N. 2007. Biostabilization of cohesive sediment beds in a freshwater wave-dominated environment. *Limnol. Oceanogr.*, 52(2). 577 – 589.
- Fedorak, P.M., Coy, D.L., Dudas, M.J., Simpson, M.J., Renneberg, A.J., MacKinnon, M.D., 2003. Microbially-mediated fugitive gas production from oil sands tailings and increased tailings densification rates. *J. Environ. Eng. Sci.* 2, 199–211.
- Fedorak, P.M., Coy, D.L., Salloum, M.J., Dudas, M.J. 2002. Methanogenic potential of tailings samples from oil sands extraction plants. *Can. J. of Microbiol.* 48(1), 21 – 33.
- Flemming, H.C. 2011. The perfect slime. *Colloids and Surfaces. B-Biointerfaces*, 86, 251 – 259.

- Froelich, P.N., Klinkhammer, G.P., Bender, M.L., Luedtke, N.A., Heath, G.R., Cullen, D., Dauphin P., Maynard, V. 1979. Early oxidation of organic matter in pelagic sediments of the eastern equatorial Atlantic: Suboxic diagenesis. *Geochimica Cosmochimica Acta.*, 43, 1075 – 1090.
- Gundersen, J.K., Jorgensen, B.B. 1990. Microstructure of diffusive boundary layers and the oxygen uptake of the sea floor. *Nature*. 345, 604–607.
- Holowenko, F.M., MacKinnon, M.D., Fedorak, P.M., 2000. Methanogens and sulphate-reducing bacteria in oil sands fine tailings waste. *Can J Microbiol.*, 46(10), 927 – 937.
- Jorgensen, B.B., Revsbech, N.P., 1985. Diffusive boundary layers and the oxygen uptake of sediments and detritus. *Limnol. Oceanogr.* 30(1), 111-122.
- Jorgensen, B.B., Des Marais, D.J. 1990. The diffusive boundary layer of sediments: Oxygen microgradients over a microbial mat. *Limnol. Oceanogr.* 35(6), 1343 – 1355.
- Lévesque, L.M.J. and De Boer, D.H., 2000. Trace element chemistry of surficial fine-grained laminae in the South Saskatchewan River, Canada. *International Association of Hydrological Sciences Publication*, 263, 183-190.
- Lorke, A., B. Müller, M. Maerki, and A. Wüest (2003), Breathing sediments: The control of diffusive transport across the sediment-water interface by periodic boundary layer turbulence. *Limnol. Oceanogr.*, 48, 2077 – 2085.
- Mehta, A.J., 1989. On estuarine cohesive sediment suspension behaviour. *J. Geophys. Res.* 94, 14303 - 14314.
- Paterson, D. M. 1997. Biological mediation of sediment erodibility: Ecology and physical dynamics. N. Burt, E. J. Prager, J. G. Southard, and E. R. Vivoni Gallart [eds.], *Cohesive sediments*. Wiley. 215 – 229.
- Penner, T.J., Foght, J.M., 2010. Mature fine tailings from oil sands processing harbour diverse methanogenic communities. *Can. J. Microbiol.* 56, 459–470.

Ramos-Padron, E., Bordenave, S., Lin, S., Mani Bhaskar, I., Dong, X., Sensen, C.W., Fournier, J., Voordouw, G., Gieg, L.M. 2011. Carbon and Sulfur Cycling by Microbial Communities in a Gypsum-Treated Oil Sands Tailings Pond. *Environ. Sci. Technol.* 45:439-446.

Stasik S., Loick N., Knoller K., Weisener C.G., Wendt-Potthoff K., 2014. Understanding biogeochemical gradients of sulfur, iron and carbon in an oil sands tailings pond. *Chem. Geology.* 382, 44-53.

Stone, M., Droppo, I.G., 1994. In-channel surficial fine-grained sediment laminae (part II): chemical characteristics and implications for contaminant transport in fluvial systems. *Hydrological Processes*, 8(2), 113 – 124.

Stumm, W. and Morgan, J.J., 1996. Aquatic Chemistry, Chemical Equilibria and Rates in Natural Waters, 3rd ed. John Wiley & Sons, Inc., New York, 1022p.

Tijhuis, L., Rekswinkel, E., van Loosdrecht, M.C.M., Heijnen, J.J., 1994. Dynamics of population and biofilm structure in the biofilm airlift suspension reactor for carbon and nitrogen removal. *Water Science and Technol.*, 29(10-11), 377 – 384.

Tolhurst, T.J., Reithmueller, P., Paterson, D.M., 2000. In situ versus laboratory analysis of sediment stability from intertidal mudflats. *Continental Shelf Res.* 20 (10/11), 1317 - 1334.

Wang, Y. H., Bohlen, W. F., O'Donnell, J. 2000. Storm enhanced bottom shear stress and associated sediment entrainment in a moderate energetic estuary. *Journal of Oceanography*, Japan, 56, 311–317.

Williams, B., 2003. Heavy hydrocarbons playing key role in peak-oil debate, future energy supply. *Oil Gas J.* 101, 20–27.

www.ags.gov.ab.ca

oilsandstoday.ca

Google maps

CHAPTER 2

PHYSICOCHEMICAL GRADIENTS, DIFFUSIVE FLUX, AND

SEDIMENT OXYGEN DEMAND WITHIN OIL SANDS TAILINGS MATERIAL FROM

ALBERTA, CANADA

2.1 Introduction

The FFT from P1A and STP were used to identify and compare the effects of oxic vs. anoxic environments on these two tailings materials, differing in age. P1A is ~35 years old, thus FFT represents aged tailings as they have already experienced consolidation within the pond. STP is a relatively young pond, only ~8 years old, thus the FFT consists of freshly processed tailings material, not yet consolidated. It is expected that the aged P1A FFT will exhibit a higher productivity and than the fresh STP FFT, since the microbial community has had sufficient time to grow, adapt and thrive in P1A. Observing the evolution of these FFT products will identify the microbial and/or chemical drivers influencing the biogeochemical alteration within these tailings environments. Further, comparing FFT from different tailings pond environments can give insight as to whether or not the overall redox chemistry and SOD varies between ponds, indicating whether all FFT products are similar or not.

In order to gain a holistic understanding of these FFT products and how they evolve temporally, laboratory microcosm-based studies have provided results giving insight into the underlying biogeochemical processes within these tailings environments. Chen et al. (2013) identified the dominant cycling of Fe and S within

WIP FFT. In this study characteristic sulfide banding was produced within the laboratory microcosms, just below the FFT-OSPW interface. Further, that study also observed rapid consumption of DO within biotic systems, indicating the dominant microbial role in the cycling of key elements such as O₂, Fe and S. These observations indicate that in the absence of oxygen, the chemically reducing conditions often observed in natural wetlands, lakes and soils is also present within the FFT of tailings ponds studied thus far. This study will look at FFT of varying age to ascertain whether or not similar biogeochemical characteristics are observed within fresh FFT and aged (consolidated) FFT products. It would be expected that materials differing in age and underlying chemical characterization would exhibit different physico-chemical trends over time, but retain the prominent attribute of the defined sulfidic zones as observed in WIP (Chen et al. 2013).

2.2 Methods

2.2.1 Laboratory Microcosms

Fluid Fine Tailings (FFT) and oil sands processed water (OSPW) samples were taken on June 7, 2012 from Pond 1A (P1A), and June 13, 2012 from Pond STP (STP) at the Suncor Energy Inc. operations site north of Fort McMurray, Alberta, Canada. P1A is classified as a “mature” pond that no longer receives FFT input, but received initial FFT materials in 1977 (~38 years in age at the time of sampling), with the overlying OSPW still being recycled for the processing circuit and extraction process. STP represents a fresh FFT waste product, with the basin in

operation for 8 years. Within this context this material is considered to be more juvenile in both its chemical and biological development, with fresh FFT and OSPW being pumped in regularly. The FFT and OSPW samples were sealed in 20L buckets and shipped and stored at 4°C until the study began.

A 2x2 factorial designed study, utilizing laboratory-based microcosms were used to compare the FFT material collected from two individual ponds (Table 2.1). The treatments included a comparison of biotic vs. abiotic treatments (distinguishing microbial vs. chemical activity) exposed to two different atmospheric conditions (see Table 2.2 for initial FFT chemical measurements). The abiotic were sterilized at the McMaster Institute of Applied Radiation Services (McIARS) in Hamilton, Ontario, Canada. The samples were irradiated for 24 hrs at 28 kGy (Chen et al. 2013). Atmospheric and anoxic exposure conditions were used to contrast the effects of oxic vs. anoxic environments (e.g. simulating zones of hypoxia at the bottom of a lake or pond). Samples for the anoxic study were kept in a moisture-controlled anaerobic chamber void of oxygen, containing ~95% N₂ and 5% H₂. All microcosms were sampled over a 52-week study period, with sampling at weeks 2, 4, 8, 16, 32 and 52.

In addition to the large 6L bioreactor described in Chen et al. 2013, a smaller column was also used measuring 4 inches in diameter. These smaller microcosms consist of replicates for increased accuracy in sampling, containing approximately 0.8L of FFT and 0.4L of OSPW, and are sacrificed at each sample period to eliminate

possible disturbance or contamination that could affect future samplings and measurements. Small microcosms are ethanol sterilized (70% ETOH) used for duplicate microsensor profiles, pore water analysis for cations and anions, microbial DNA studies (future publication), and future mineralogical classification. The ethanol sterilized, 4L Camwear^R containers from the Cambro Manufacturing Company are also used for microsensor profiling over the 52-week period, as well as headspace gas sampling. Those used solely for headspace gas sampling are fitted with a rubber o-ring around the lid, and ports to allow gas extraction via sterile gas-tight syringes. The large microcosms (also ethanol sterilized; 70% ETOH) contain approximately 2L of FFT and 1L of OSPW. Anoxic microcosms followed the same procedure as set out in Chen et al. 2013, being flushed with ultra pure N₂, then cycled again with 95% N₂, 5% H₂ within the anoxic chamber. All microcosms were kept at room temperature (22 °C), in complete darkness.

2.2.2 Microsensor chemical profiles

Microelectrode sensors (Unisense Science, Denmark) were used to measure HS⁻, O₂, pH, and Eh gradients vertically across the FFT-OSPW interface (Revsbech, 1989; Elberling and Damgaard, 2001; Sorensen et al., 2009). These sensors are used via a computer controlled micro-manipulator (Figure 2.1), measuring at intervals of 1 mm, from ~20 mm above the FFT-water interface to depths of (or greater than) 50 mm into the FFT. The data is recorded via SensorTrace Pro software in connection with the Unisense Microsensor Multimeter, a multi channel laboratory amplifier.

The microsensors used in this study are glass tipped and range in size from 100-500 μm (depending on sensor).

2.2.3 Diffusivity calculations and chemical flux

Diffusivity measurements across the water-FFT interface were measured using O_2 and HS^- microsensor algorithms where the slope of the concentration gradient was used to compute the corresponding flux values (Chen et al. 2013). A 50 μm Unisense glass tip diffusivity sensor was used in this case to compare diffusivity coefficients recorded across the OSPW-FFT interface for each pond (P1A and STP) and each treatment (biotic and abiotic). A two-point calibration was performed prior to measurement as stated in Revsbech et al. 1998. These FFT-specific coefficients are used with O_2 and HS^- concentration profiles for the respective microcosm. The flux of O_2 and HS^- is calculated according to Fick's first law of diffusion:

$$J(x) = -\phi D(x) \frac{dC(x)}{dx} \quad (1)$$

where $J(x)$ is the diffusion flux; $-\phi D(x)$ is the apparent diffusivity as measured by the Unisense diffusivity sensor (porosity*diffusion coefficient); and $dC(x)/dx$ is the slope of the concentration profile (Revsbech et al. 1998). The final flux measurement represents the amount of molecules of a specific substance moving from a location of high concentration to low concentration, per unit area per unit time. Both the OSPW and FFT are relatively homogenous, therefore assumptions made for Fick's first law are in this case appropriate for use in this study.

2.2.4 Gas expression

Headspace gas was extracted in duplicate from the large, sealed microcosms using gas-tight syringes attached via three-way valve to a port on the top of each microcosm. The 5ml gas sample was injected into a glass vial filled with helium-de-oxygenated water and crimped-capped with a chromatography specific septa. The vial is allowed to reach equilibrium pressure by expelling 5ml of the water through an open-ended needle. These samples were run using a gas chromatography in 20 μ l aliquots for analyses of HS^- and CH_4 . The GC was a Variant CP3800 equipped with a Thermal Conductivity Detector (TCD), with an HP column (part # 19095p-Q04). The GC was set at an oven temperature of 90°C, column temperature of 95°C, with a column flow rate of 1.3 ml min⁻¹ for all samples injected. HS^- and CH_4 standards were run in tandem with headspace samples to ensure accuracy and precision.

2.3 Results and Discussion

2.3.1 Biogeochemical alteration of FFT materials

This study was designed to investigate the effects of both chemically and biologically driven processes on the biogeochemistry of two tailings ponds from Suncor Energy Inc. These pond materials were divided into 8 total treatments based on pond type and environmental condition. Here we define microcosms containing the freshly processed STP materials and aged P1A materials as: **STP_{OXBIO}** and **P1A_{OXBIO}**, representing biotic (non-sterilized) FFT in *atmospheric* conditions for the respective pond material; and **STP_{ANBIO}** and **P1A_{ANBIO}** representing biotic (non-sterilized) FFT in *anoxic* conditions for the respective pond material. Further,

STP_{OXCON} and **P1A_{OXCON}** represent the abiotic (sterilized) control materials in *atmospheric* conditions for the respective pond; while **STP_{ANCON}** and **P1A_{ANCON}** represent the abiotic controls in the *anoxic* environment for the respective pond materials. Experimental protocols can be found in section 2.1 of Materials and Methods.

The physico-chemical alteration within the laboratory microcosms was observed and monitored on a weekly basis over a 52-week period. Figure 2.2 shows an illustration of the reactions at week 16. All of the oxic biotic microcosms showed visible orange coloration starting between 2 and 4 weeks for P1A_{OXBIO} and at 8 weeks for STP_{OXBIO}, suggesting the formation was resulting from the oxidation of ferrous iron present in the FFT matrix. Note that none of the sterile controls in this study showed visible evidence of iron oxidation exposed to atmospheric conditions used in this study. This suggests that in part, this transformation is influenced by the microbiology present within the systems studied. By comparison, the biotic microcosms of both P1A and STP exposed to anoxic conditions exhibited black discoloration within the individual FFT materials investigated. It is interesting to note that the iron sulfide bands that were observed in the individual microcosm treatments initially formed at the interface for all P1A_{ANBIO} FFT materials studied and slowly consumed the entire FFT in a top-down manner. In contrast the STP_{ANBIO} FFT formed initial iron sulfide bands at the base of the FFT, progressing from the bottom to the middle of the microcosm. From a microbial perspective, the observed diagnostics noted for these microcosms resemble classic facultative anaerobic versus obligate anaerobic behavior respectively. These results compare favorably

with the WIP microcosms studied by Chen et al., (2013) who observed a similar dark band formation, which was attributed to the gradual increase, and formation of iron mono sulfides within the FFT matrix. Again, there was no color change observed in the sterilized control samples under anoxic conditions, suggesting that the resulting processes in P1A_{ANBIO} and STP_{ANBIO} are driven by the biotic cycling of Fe and S, and Fe and O₂ in both P1A_{AXBIO} and STP_{AXBIO}.

It was also noted that consolidation of the FFT over the 52-week period occurred rapidly in the STP_{AXBIO} and STP_{ANBIO} microcosms (see Figure 2.3) indicative of microbially mediated processes, accelerating the consolidation of FFT, studied in several other tailings systems (e.g. Voordouw, 2012; Holowenko et al., 2000; Fedorak et al., 2003; Siddique et al., 2014). All of the aged P1A FFT experienced negligible settling and consolidation during the 52 weeks, since it had experienced significant consolidation prior to the experiment. By the end of the 52-week study, the amount of consolidation for both the control (sterile) and biotic STP FFT systems were similar despite microbial contributions, manifesting the same end result, although at a faster rate compared to physical gravitational driven processes in the abiotic STP FFT materials.

2.3.2. Dissolved Oxygen

Dissolved O₂ concentration was measured across the FFT-OSPW interface over 52 weeks for the representative microcosm experiments. Both STP_{AXBIO} and P1A_{AXBIO} microcosms measured constant DO concentrations of $5.75 \pm 0.335 \text{ mg L}^{-1}$ and $6.57 \pm 0.556 \text{ mg L}^{-1}$ respectively, over the 52 week period under normal

atmospheric conditions. These results correlate with Chen et al. (2013), where initial OSPW concentrations in oxic biotic WIP were measured at 6.8 mg L^{-1} decreasing to 5.4 mg L^{-1} by 52-weeks in that study. The DO measurements across all biotic FFT interfaces showed rapid O_2 consumption decreasing to 0 mg L^{-1} at 2-3 mm for both the $\text{P1A}_{\text{OXBIO}}$ FFT and $\text{STP}_{\text{OXBIO}}$ FFT just below the interface. In contrast, the OSPW of the $\text{P1A}_{\text{OXCON}}$ microcosm had a measured DO of $6.51 \pm 0.395 \text{ mg L}^{-1}$, while the $\text{STP}_{\text{OXCON}}$ OSPW was $8.25 \pm 0.0167 \text{ mg L}^{-1}$. The reason for the higher DO concentrations in the sterile control systems could be related to the lack of biological activity resulting from direct microbial respiration at the FFT-water interface as observed by Chen et al. (2013). Similar trends were observed for DO concentrations profiles below the FFT-water interface. In both $\text{P1A}_{\text{OXCON}}$ and $\text{STP}_{\text{OXCON}}$ FFT, progressive diffusion of DO into the FFT was observed with time as stated by Chen et al. (2013).

In the anoxic environment, $\text{P1A}_{\text{ANBIO}}$ and $\text{STP}_{\text{ANBIO}}$ measured cap water O_2 concentrations below 1 mg L^{-1} approximately 4 weeks into the study (extreme , as all residual O_2 was actively being consumed. Furthermore, consumption of O_2 across the FFT-water interface was immediate in all biotic microcosms in less than 2 weeks, with O_2 reaching 0 mg L^{-1} . Similar trends of DO behavior were observed by Chen et al. (2013) for their anoxic treatments. Rapid consumption of DO was observed just days after setting up the microcosms.

2.3.3. *HS⁻ production*

One of the most dominant processes within sediments and FFT environments is the reduction of sulfate, coupled with the production of sulfides. Average sulfate (SO_4) concentrations were measured in initial bulk FFT materials from STP and P1A (Table 1.2), measuring the available sulfate pool at the beginning of this study. STP FFT contained the highest average concentration of SO_4 at 252.8 mg L^{-1} , followed by P1A FFT at 41.8 mg L^{-1} , just 16.5% of that measured in STP. In comparison, WIP FFT measured only $7.8 \text{ mg L}^{-1} \text{ SO}_4$ (Chen et al., 2013), obviously significantly lower than the above concentrations measured in STP and P1A.

Measurements of HS^- concentrations were performed under both atmospheric and anoxic conditions. HS^- profiles from the FFT-water interface to 50 mm into the FFT were performed. The $\text{P1A}_{\text{OXBIO}}$, $\text{P1A}_{\text{OXCEN}}$, $\text{STP}_{\text{OXBIO}}$ and $\text{STP}_{\text{OXCEN}}$ microcosms measured negligible HS^- within the FFT for the duration of this study, the opposite of what was observed in Chen et al. (2013). Here the authors noted that the oxic biotic WIP microcosms measured an excess of $150 \text{ } \mu\text{mol L}^{-1} \text{ HS}^-$ at 2.5 mm into the FFT, despite the lowest measured pore water sulfate concentrations explained above. The highest recorded HS^- concentrations in this study were observed at week 32 in the $\text{P1A}_{\text{ANBIO}}$ microcosms, with HS^- measuring $5 \text{ } \mu\text{mol L}^{-1}$ at 50 mm depth, while $\text{STP}_{\text{ANBIO}}$ peaked at $3 \text{ } \mu\text{mol L}^{-1}$ at week 16. The onset of HS^- formation is linked to the development of moderate reducing conditions observed in P1A FFT ($\text{Eh } -171 \text{ mV}$) and STP FFT ($\text{Eh } -112 \text{ mV}$). At week 52, all anoxic sterile controls still measured $<1 \text{ } \mu\text{mol L}^{-1} \text{ HS}^-$. At this same time, HS^- concentrations declined in the biotic anoxic systems, with concentrations decreasing to $4.4 \text{ } \mu\text{mol L}^{-1}$

in P1A_{ANBIO} and STP_{ANBIO} reaching only 2 $\mu\text{mol L}^{-1}$ at 50mm below the interface, well within the sulfidic zone of coloration noted above. Overall, the HS⁻ concentrations measured within the FFT for P1A_{ANBIO} and STP_{ANBIO} microcosms are just 3.3% and 2% of the peak measurements of WIP FFT respectively. In addition, the concentration in WIP only decreased to an equilibrium of 27 $\mu\text{mol L}^{-1}$ for the remainder of that study, still considerably more than anything measured in P1A or STP (Chen et al., 2013). This variation in results indicates that these ponds differ in terms of productivity, likely due to the indigenous microbial consortia such as sulfide reducing bacteria, as well as the bulk chemical characteristics of the FFT (see Table 2.2). These authors suggest that perhaps the produced HS⁻ in P1A and STP is being more rapidly sequestered in FeS minerals than in WIP, indicated by the rapid black discoloration observed (see 3.1).

2.3.4. Oxygen and Hydrogen Sulfide Diffusivity and flux

2.3.4.1 Apparent Diffusivity measurements for P1A and STP FFT

The apparent diffusivity (porosity*diffusivity coefficient) was measured for P1A FFT and STP FFT and are compared to those noted in WIP FFT measured by Chen et al. (2013) (Table 2.3). Further details on the calculation of apparent diffusivity using the Unisense Diffusivity sensor are outlined in 2.3. STP_{ANBIO} and STP_{ANCON} showed the highest apparent diffusivities of $2.11 \times 10^{-5} \text{ cm}^2 \text{ s}^{-1}$ and $2.21 \times 10^{-5} \text{ cm}^2 \text{ s}^{-1}$ respectively, while P1A_{ANBIO} measured a slightly lower apparent diffusivity of $1.61 \times 10^{-5} \text{ cm}^2 \text{ s}^{-1}$, followed by $7.56 \times 10^{-6} \text{ cm}^2 \text{ s}^{-1}$ in P1A_{ANCON}. The higher apparent diffusivities measured in STP FFT correlates with the very *liquid*

nature of the STP FFT slurry, as very little consolidation has taken place to this point. Since the apparent diffusivity is directly correlated to the porosity of the medium, the process of consolidation will lower porosity, therefore decreasing apparent diffusivity. Thus, the lower apparent diffusivity measured in the P1A FFT, is likely attributed to the age of the material, since consolidation over time has decreased the rate of molecular diffusion through the FFT. However, taking into account diffusion coefficients of WIP (Chen et al. 2013) and those of sulfide mine tailings (Elberling & Daamgaard, 2001), a much higher coefficient was measured. This suggests that the WIP mineralogy is very diffuse in nature (i.e. larger pore spaces), or the formation of iron-sulfide minerals in this FFT may have opened up diffusion pathways for more efficient diffusion of molecules through mineral pore spaces. In addition, the biotic P1A apparent diffusivity is approximately double that measured in the sterile control, again indicating the presence of sulfide minerals may have also increased its diffusive nature.

2.3.4.2 Dissolved Oxygen Flux

The calculated DO flux (Table 2.4) was measured across FFT-water interfaces into the FFT and were determined for the atmospheric treatments. The highest DO flux for STP_{OXBIO} was 7.52 mmol m⁻² day⁻¹ at week 2, which steadily decreased to 4.46 mmol m⁻² day⁻¹ by week 52 and is likely related to the extensive settling/consolidation of solids. P1A_{OXBIO} on the other hand showed comparable O₂ fluxes, from 3.20 mmol m⁻² day⁻¹ at week 2 to 3.29 mmol m⁻² day⁻¹ at week 52, suggesting a quasi state of equilibrium from the perspective of DO flux for this FFT

material, over a year of monitoring. The decreasing trend of DO flux observed in STP FFT is partially attributed to its noted consolidation, since it reduces the potential for O_2 to easily diffuse past the FFT-water interface. Additionally, the production of reduced compounds, further consuming available O_2 , could also account for the decreasing DO flux over time, since measured DO concentrations ~ 2 mm past the interface were 0 mg L^{-1} just days after setting up the microcosms (see 3.2). The relatively stable DO flux observed in P1A_{OXBIO} is representative of the aged P1A FFT material (~ 36 y), since the tailings have undergone prior consolidation. Comparing biotic to abiotic treatments, it is clear the SOD is driven by the biological processes in all ponds, with the exception of week 52 noted for STP_{OXCON} and WIP_{OXCON} (Chen et al., 2013). In this case, the authors attribute the increased abiotic DO flux to be based on the chemically driven exhaustion of reducible compounds (Melton et al., 2014), facilitating active DO diffusion into the FFT material. In summary, a hierarchy in DO flux can be observed, with STP being most diffuse across the FFT-OSPW interface, followed by P1A then WIP (Chen et al. 2013).

When comparing measured DO flux to natural freshwater lake and marine settings (Table 2.5), measured laboratory concentrations are lower than what may be expected in natural systems. A shallow freshwater lake in Switzerland measured a nighttime DO flux of $35 \text{ mmol m}^{-2} \text{ day}^{-1}$ (McGinnis et al., 2008), while a subarctic lake in Iceland measured higher DO flux of $89 \text{ mmol m}^{-2} \text{ day}^{-1}$ (Thorbergdottir et al., 2004). Perhaps the most similar DO fluxes were measured on various continental shelves, with measurements ranging from $1.5 \text{ mmol m}^{-2} \text{ day}^{-1}$ to as high as $42 \text{ mmol m}^{-2} \text{ day}^{-1}$ (Giles et al., 2007). However, the laboratory-based

microcosms in this experiment do not experience natural disturbances, such as winds, waves and movement of benthic organisms, limiting the natural diffusion of DO through the water column, past the FFT-OSPW interface (Revsbech et al., 1980; Andersen and Helder, 1987). Such disturbances would undoubtedly increase DO influx into the water column, in turn increasing DO flux (Aller, 1983; Forster and Graf, 1992; Forster and Graf, 1995). Further, the very act of pumping large amounts of tailings in and out of the tailings ponds will create aeration with atmospheric oxygen, further increasing oxygen influx in the actual tailings pond. However, this lab-based approach still provides an accurate representation of expected values in controlled environments, and perhaps are similar to those where no in/outflow is experienced in future EPLs or reclaimed wetlands.

2.3.4.3 Hydrogen Sulfide Flux

Hydrogen sulfide (HS^-) flux (Table 2.6) was measured in the anoxic treatments. No measurable HS^- was observed under atmospheric conditions. The fluxes for all P1A and STP FFT were calculated from the measured HS^- gradient, from 10-40 mm below the FFT-OSPW interface, and the measured apparent diffusivities (Table 2.3). No detectable HS^- was measured in the abiotic systems, thus no flux could be calculated. The HS^- flux (Table 2.6) reported for $\text{STP}_{\text{ANBIO}}$ FFT is $0.04 \mu\text{mol m}^{-2} \text{ day}^{-1}$ at week 2, reaches a maximum of $6.25 \mu\text{mol m}^{-2} \text{ day}^{-1}$ at week 20 and then decreases to $2.61 \mu\text{mol m}^{-2} \text{ day}^{-1}$ at week 52. $\text{P1A}_{\text{ANBIO}}$ on the other hand, reaches a maximum HS^- flux of $37.6 \mu\text{mol m}^{-2} \text{ day}^{-1}$ at week 2, decreasing to $10.9 \mu\text{mol m}^{-2} \text{ day}^{-1}$ at week 20, then decreasing further to $7.12 \mu\text{mol m}^{-2} \text{ day}^{-1}$ by

week 52. The enhanced flux in P1A compared to STP suggests that other factors may be stimulating this response, such as a more active SRB microbial community generating this HS^- . Further, the slightly alkaline pH of ~ 8.1 , and the dark black coloration is indicating FeS mineralization within P1A_{ANBIO}. This explains the decreasing trend in sulfide flux over the 52-week study, as increasing quantities of HS^- are sequestered in sulfide minerals (as mentioned in 3.1). Again is most evident in the aged P1A FFT, compared to the fresh STP FFT. In comparison to peak HS^- flux measured in WIP (Chen et al., 2013) ($278 \mu\text{mol m}^{-2} \text{ day}^{-1}$), the maximum flux measurements in this study for STP_{ANBIO} and P1A_{ANBIO} are just 2.2% and 13.5% of that of WIP respectively, leading to a general hierarchy of HS^- flux led by WIP, followed by P1A then STP. WIP HS^- flux peaks at the same time as P1A (week 2), then steadily decreases, suggesting that the sulfate pool is being steadily depleted during the course of both studies. Further, Chen et al. (2013) showed an increase in framboidal pyrite (FeS) grains after 36 weeks in their anoxic microcosms, corroborating the findings from this study. These results are also supported in a microcosm study by Bethke et al. (2011). In that study of alluvial aquifer sediments (representing limited energy environments) produced sulfides where nearly completely sequestered in precipitated FeS minerals.

Compared to freshwater and marine environments (table 2.7) – essentially systems from freshwater and salt-water environments – the measured sulfide fluxes of STP and P1A again measure in the lower range of average marine settings but are similar to values measured in freshwater lakes of the Canadian Shield (Richards et al., 1991). Fluxes measured in the Santa Barbara Basin as well as the continental

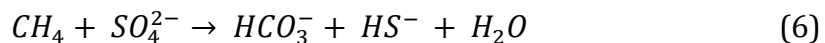
shelf upwelling off the Namibia coast show sulfide fluxes ranging from $10^1 - 10^3$ higher than those measured in the FFT of this study (Kuwabara et al., 1999; Bruchert et al, 2003). WIP HS^- fluxes ($278 \mu\text{mol m}^{-2} \text{ day}^{-1}$) are also quite high, and are comparable to those of the Santa Barbara basin, reaching close to the measured upper limit of $312 \mu\text{mol m}^{-2} \text{ day}^{-1}$ (Chen et al., 2013; Kuwabara et al., 1999). Comparison of conductivity and pH values between the two Suncor ponds (Table 2.2) indicates that the higher salinity coupled with lower pH of WIP are more comparable to these marine environments. This comparably higher salinity in WIP perhaps explains its HS^- flux similarity to the Santa Barbara Basin, in that this salinity has some affect on this sulfide flux. P1A on the other hand has a conductivity of $\sim 1500 \mu\text{S/cm}$, which is comparably lower than the $3550 \mu\text{S/cm}$ measured in WIP (Chen et al. 2013). Pond STP, with a conductivity of $\sim 3500 \mu\text{S/cm}$, similar to that of WIP, may evolve to closely mimic characteristics WIP in the future, given sufficient consolidation.

2.3.5 Headspace methane expression

Headspace gas evolution was monitored for the closed anoxic microcosms over the 52-week period. All STP samples measured no detectable methane, with concentrations being below the detection limit (BDL). Methane concentrations measured for P1A_{ANBIO} and P1A_{ANCON} microcosms showed opposite trends (Figure 2.4). The P1A_{ANBIO} microcosm measured an initial concentration at week 2 of 0.2 % CH_4 in N_2 (standard temperature and pressure). However, from week 4 to week 52, methane was not detectable. Measured headspace CH_4 concentrations in the

headspace of P1A_{ANCON} yielded unexpected results. Concentrations in the headspace at week 2 were 2.1 % CH₄ in N₂, increasing linearly to 13.9 % CH₄ in N₂ at week 52. Despite the sterilized state of the P1A_{ANCON} FFT, this expulsion of CH₄ into the headspace was observed through the duration of the study, at a rate of +0.034 % CH₄ day⁻¹.

The trends measured in P1A_{ANBIO} are indicative of the competition between thriving SRB communities, and possibly outcompeting or suppressing methanogenic activity resulting in less CH₄ production from the FFT source. Furthermore, the lack of detectable H₂S and CH₄ suggest that both SO₄/HS⁻ and CO₂/CH₄ respiration could be in equilibrium over the 52-week period monitored, and any CH₄ was likely oxidized by other reactants stimulated by the microbial consortia (ANAerobic MEthanotrophs – ANME), before it passed into the headspace (Knittel and Boetius, 2009). This mechanism, though not yet fully understood has been discussed in several studies by Knittel and Boetius (2009), Haroon et al. (2013) and Joye et al. (2004) who suggest that produced CH₄ can be oxidized prior to release into headspace (closed systems) or the atmosphere, and is termed the anaerobic oxidation of methane (AOM). This CH₄ oxidation co-exists with the reduction of sulfate where the mechanism for the AOM follows equation 6 (Knittel and Boetius (2009)):



Bethke et al. (2011) further showed that methanogenesis and sulfate reduction work simultaneously, and was not dependent necessarily on a thermodynamic hierarchy, which could certainly be applied to observations in P1A FFT. Methane could be oxidized by residual sulfate or other potential oxidants in the FFT, resulting in the production of bicarbonate and sulfide. However, these chemical products can be quickly altered again, thus indicating why measured alkalinity (results not shown) decreased over time, instead of leading to an increase in alkalinity as one would expect from an HS^- generating reaction (Giblin et al., 1990).

The interesting results of P1A_{ANCON}, measuring increasing concentrations of CH_4 over time go against what would be expected from a sterile control system. We suggest that this increase in headspace methane concentration within this microcosm is a result of residual methane released from the pore waters that had accumulated in the consolidated FFT prior to sample collection. The expulsion of residual CH_4 from the pore spaces was likely caused in part due to the sterilization of the FFT, in that the methane oxidizing methanotrophs were eliminated, thus allowing the methane to pass into the headspace. Voordouw (2013) indicated that there are large quantities of methane known to exist, trapped in heavily consolidate tailings environments. One such study, for example, suggested methane comprised 2-5% total volume of Mildred Lake Settling Basin (Holowenko et al., 2000), another aged tailings pond in Alberta, Canada.

2.4 Conclusions

This study has provided insight into the possible biogeochemical processes influencing the chemical flux of O_2 and HS^- at the FFT-OSPW interface and methane expression behavior for a range of aged FFT products from the Athabasca Oil Sands. Previous studies have identified important chemical cycles and microbial community structures in various pond environments, but direct comparison between ponds of different underlying characteristics where lacking (Chen et al. 2013). Elucidating parameters contributing to the physico-biogeochemical function within these FFT products and behaviors across the FFT/OSPW interface is paramount for establishing their long-term stability and eventual rehabilitation. The study has provided direct correlation and determined flux estimates for factors controlling the overlying water column, with direct implication on the FFT_{SOD} for two different operationally defined FFT products. The biologically driven carbon degradation process is a contributing factor in all processes observed in this study, especially evident in the biogeochemical alteration observed between microcosms due to the presence of O_2 in the atmospheric systems, and no O_2 within the anoxic treatments. This investigation corroborates the Chen et al. (2013) study, which showed similar reaction kinetics with respect to sulfur and DO flux across the FFT-OSPW interface. In addition the current investigation determined that the measured gas concentrations of H_2S and CH_4 in P1A and STP FFT microcosm headspace is directly linked to biological activity and/or composition. In this case the probable presence of SRB and ANME bacteria are obviously limiting the expression of these harmful gases into the atmosphere, by quickly sequestering these compounds

within the upper FFT matrix. The observed decrease in flux for HS^- supports this self-limiting assumption for S within the STP and P1A tailings environments. This will be crucial for future development plans and maintaining sustainable environments in areas incorporating these FFT materials. In addition, it is clear from this study that STP, P1A and WIP FFT materials (Chen et al., 2013) are all unique from a biogeochemical response perspective (e.g. the flux relationships) but do share obvious similarities with respect to their tendency to form stratified REDOX conditions. Further, definite microbial community variations have been observed between ponds (future companion publication). This corroborates some observations in this study, and is partially attributed to the maturity of the pond, leading to more diverse and facultative communities within older FFT materials (i.e. P1A). The physico-chemical data and flux measurements recorded during the duration of this study for the two FFT products will contribute to an expanding database which can be applied to both conceptual and numerical models used to predict the behaviors of FFT products used in EPLs and natural wetlands. Future studies need to include field-based approaches, which can provide both temporal and spatial context across the FFT reservoirs. In addition greater emphasis is needed to provide baseline metrics for similar systems being proposed (e.g. reference sites). These expanded field studies would give great insight into how these systems truly evolve in the “uncontrolled” natural environment. This study has shown that laboratory techniques are quite useful in determining FFT variability as a function of pond type and operating history, and how alteration over time can influence FFT chemical response prior to reclamation. Implementing techniques to

study the effects of hydrodynamic forces on the FFT-OSPW would further improve the growing database of parameters characterizing these various tailings environments, and is explored further in Chapter 3 of this thesis.

Figure 2.1 Microsensors attached to micromanipulator to measure chemical gradients vertically through the FFT-water interface within the microcosm

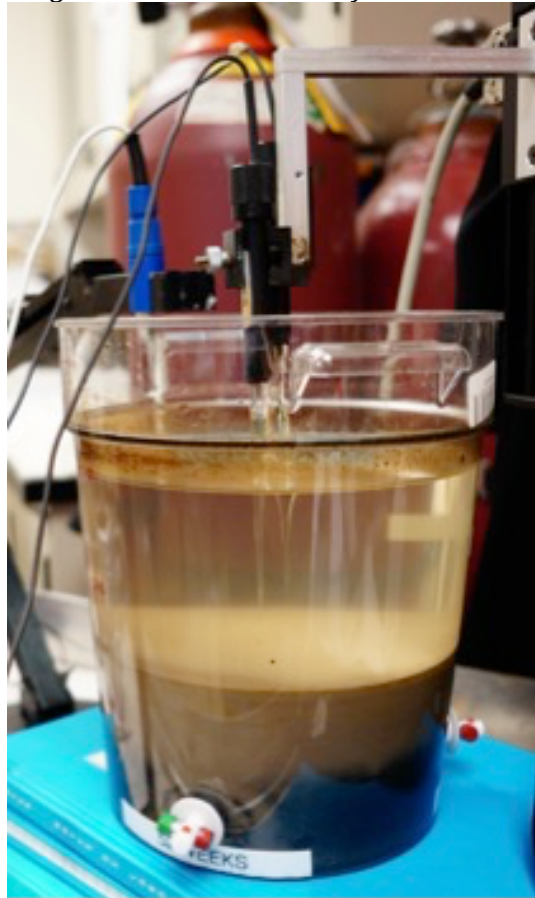


Figure 2.2: Visible physical alteration of FFT from P1A in Oxic (left) and anoxic (right) environments

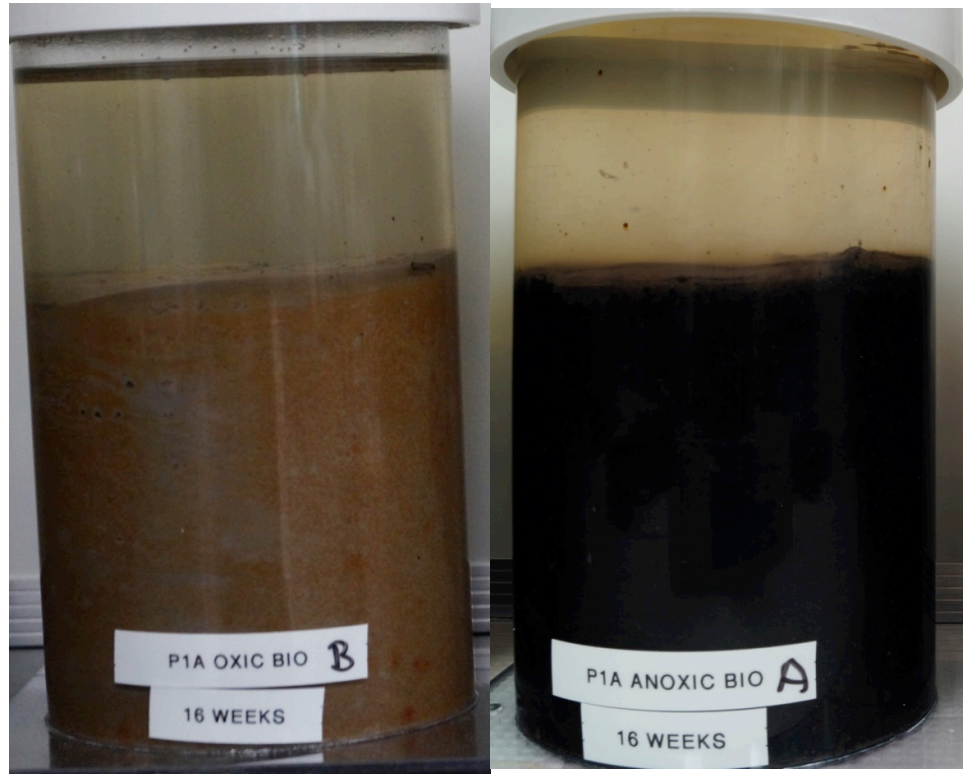


Figure 2.3: Example of the rapid initial consolidation of STP_{BIOTIC} from Week 1 to week 16. Measured settling at the interface was ~ 30 mm during this time.

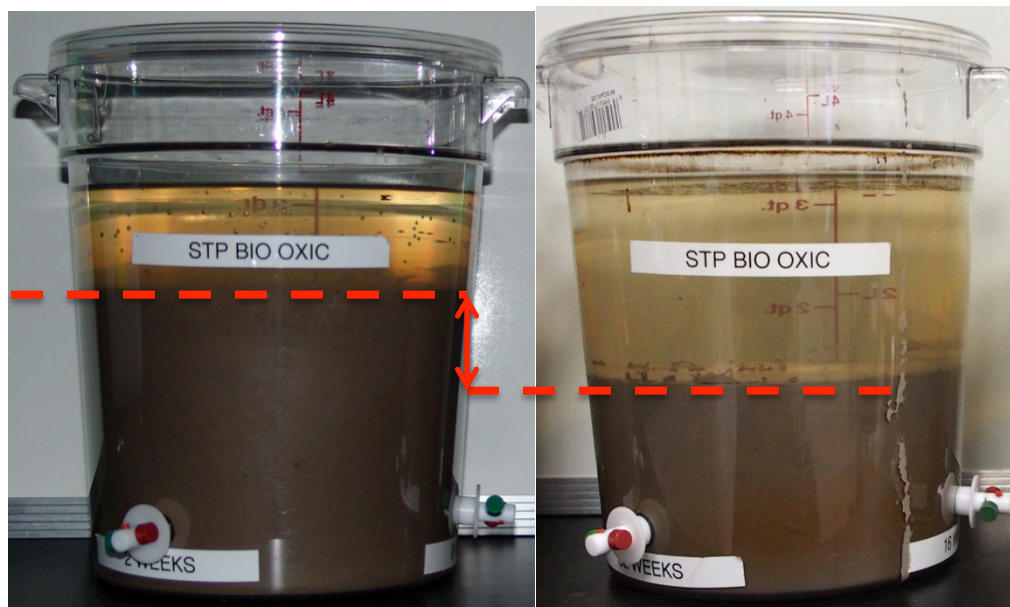


Figure 2.4: Headspace methane concentrations from anoxic P1A biotic and abiotic microcosms.

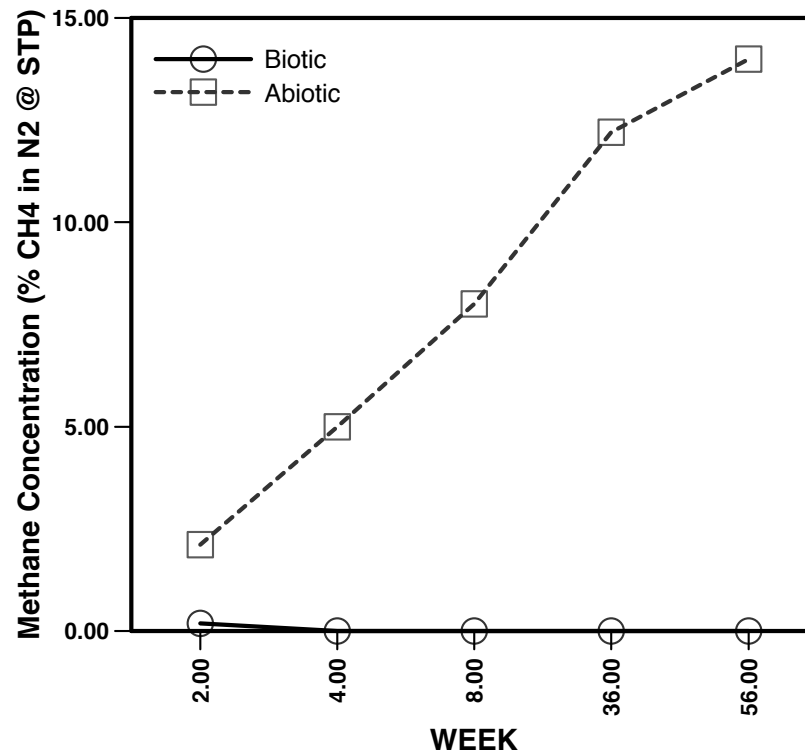


Table 2.1: Experimental design comparing two tailings pond FFTs, exposed to both oxic and anoxic conditions over the course of 52 weeks.

STP (fresh FFT)		P1A (mature FFT)	
<i>OXIC</i>	<i>ANOXIC</i>	<i>OXIC</i>	<i>ANOXIC</i>
Biotic	Biotic	Biotic	Biotic
Abiotic	Abiotic	Abiotic	Abiotic

Table 2.2: Description of bulk FFT material from P1A, STP and WIP, performed by Syncrude research laboratories before (biotic) and after (abiotic) gamma irradiation for sterilization. ^a(Chen et al. 2013)

	FFT Initial Chemistry					
	P1A		STP		WIP ^a	
	Biotic	Abiotic	Biotic	Abiotic	Biotic	Abiotic
Solid (%)	36.3		32.4		33.4	
Water (%)	57.4		66.3		64.7	
Bitumen (%)	5.5		1.4		2.0	
Conductivity (uS/cm)	1498	1646	3380	3840	3550	3200
pH	8.4	8.4	8.7	8.7	7.8	8.2
<i>Anions (mg L⁻¹)</i>						
CO ₃	16.0	15.0	23.5	24.0	123.0	137.0
HCO ₃	1380.0	1395.0	984.0	945.5	1250.0	1190.0
CaCO ₃	1155.0	1170.0	843.5	816.0	NA	NA
F	1.9	2.4	2.3	2.4	BDL	BDL
Cl	55.5	51.0	660.0	650.0	570.0	580.0
NO ₂	BDL	BDL	BDL	BDL	BDL	BDL
NO ₃	0.3	BDL	BDL	BDL	BDL	BDL
PO ₄	BDL	BDL	BDL	BDL	BDL	BDL
SO ₄	61.4	22.3	251.0	254.5	3.4	12.2
Br	BDL	BDL	0.8	0.7	BDL	BDL
<i>Cations (mg L⁻¹)</i>						
Ca	6.0	6.0	6.0	6.0	21.7	20.2
K	20.1	20.1	16.0	16.7	16.6	17.9
Mg	13.9	12.8	7.9	8.1	12.3	11.7
Na	520.5	495.0	865.0	832.5	863.0	866.0
NH ₄	20.8	21.0	5.3	5.7	10.4	13.4
<i>Trace Elements (mg L⁻¹)</i>						
Al	0.6	0.2	2.8	9.1	0.1	0.7
B	4.6	4.4	4.0	3.8	4.2	3.5
Ba	0.1	0.1	BDL	BDL	0.5	0.5
Cd	BDL	BDL	BDL	BDL	BDL	BDL
Co	BDL	BDL	BDL	BDL	BDL	BDL
Cr	BDL	BDL	BDL	BDL	BDL	BDL
Cu	BDL	BDL	BDL	BDL	BDL	BDL
Fe	0.1	0.1	0.5	1.8	BDL	0.2
Li	BDL	BDL	BDL	BDL	BDL	BDL
Mn	BDL	BDL	BDL	BDL	0.1	0.0
Mo	0.1	0.2	0.2	0.2	BDL	BDL
Ni	BDL	BDL	BDL	BDL	BDL	BDL
P	BDL	BDL	BDL	BDL	BDL	BDL
Pb	BDL	BDL	BDL	BDL	BDL	BDL
S	26.2	11.4	89.1	86.6	5.1	7.0
Sb	BDL	BDL	BDL	BDL	BDL	BDL
Se	BDL	BDL	BDL	BDL	BDL	BDL
Si	8.6	7.4	8.0	17.5	6.3	5.8
Sr	0.6	0.6	0.4	0.4	0.8	0.7
Ti	BDL	BDL	BDL	0.0	0.0	0.0
V	BDL	BDL	BDL	BDL	0.0	0.0
Zn	0.0	0.0	0.0	0.0	BDL	BDL
Zr	BDL	BDL	BDL	BDL	BDL	BDL

Table 2.3: Apparent diffusivity just below the FFT-water interface of each material.

Study	Material	Apparent Diffusivity (cm ² s ⁻¹)	
		Biotic	Abiotic
Reid et al. 2015	STP FFT	2.11 x 10 ⁻⁵	2.21 x 10 ⁻⁵
	P1A FFT	1.61 x 10 ⁻⁵	7.56 x 10 ⁻⁶
Chen et al. 2013	WIP	6.73 x 10 ⁻⁴	ND
Elberling & Daamgaard 2001	Sulfide mine tailings	3.99 x 10 ⁻⁴	ND

Table 2.4: DO flux measurements for STP, P1A and WIP (Chen et al. 2013).

Species	Pond/FFT	Time (week)	FFT flux (mmol m ⁻² day ⁻¹)	
			Biotic (BOD + COD)	Abiotic (COD)
Oxygen(DO)	STP	2	7.52	2.88
	STP	20	6.76	3.12
	STP	52	4.46	4.68
	P1A	2	3.20	1.71
	P1A	20	5.10	1.38
	P1A	52	3.29	2.24
	WIP	2	2.32	2.36
	WIP	24	4.63	1.99
	WIP	52	1.78	5.90

Table 2.5: O₂ flux measurements from natural freshwater lakes and marine environments

Location	Geographic Setting	O ₂ Flux [mmol m ⁻² day ⁻¹]
Lake Wohlen, Switzerland ¹	Shallow freshwater lake (night)	35
Lake Myvatn, Iceland ²	Highly productive subarctic lake	89
SW Netherlands ³	Estuarine intertidal sediment	22
NE New Zealand ⁴	Continental shelf	3 → 29
Others (n=30) ⁴	Continental shelf	1.5 → 42

¹McGinnis D.F. et al., (2008); ²Thorbergdottir I.M. et al., (2004); ³Hofman P.A.G. et al., (1991); ⁴Giles H. et al., (2007)

Table 2.6: Sulfide flux measurements from Pond STP, Pond 1A and WIP (Chen et al., 2013).

Species	Pond/FFT	Time (week)	HS ⁻ FFT flux ($\times 10^{-3}$ $\mu\text{mol m}^{-2} \text{ day}^{-1}$)	
			Biotic BSOD	Abiotic CSOD
Sulfide (HS ⁻)	STP	2	0.04	0
	STP	20	6.25	0
	STP	52	2.61	0
	P1A	2	37.6	0
	P1A	20	10.9	0
	P1A	52	7.12	0
	WIP	2	278	0
	WIP	6	266	0
	WIP	52	-	-

Table 2.7: Sulfide flux measurements from natural marine and freshwater environments.

Location	Geographic Setting	HS ⁻ Flux [$\mu\text{mol m}^{-2} \text{ day}^{-1}$]
Santa Barbara Basin ¹	Marine basin	0.096 \rightarrow 312
Central Namibia Coast ²	Continental shelf upwelling *very high production zone	500 \rightarrow 32000
Lake 302S ³	Canadian shield (5.1m deep)	0.4
Lake 239 ³	Canadian shield (10.5m deep)	0.32
Lake 114 ³	Canadian shield (1.7m deep)	3.9

¹Kuwabara et al. (1999) ; ²Bruchert et al. (2003) ; ³Richards, Kelly and Rudd (1991)

2.5 References

- Aller, R.C., Yingst, J.Y., Ullman, W.J. 1983. Comparative biogeochemistry of water in intertidal *Onuphis* (Polychaeta) and *Upogebia* (Crustacea) burrows: temporal patterns and causes. *J. Mar. Res.*, 41, 571 – 604.
- Andersen, F. D., Helder, W. (1987). Comparison of oxygen microgradients, oxygen flux rates and electron transport system activity in coastal marine sediments. *Mar. Ecol. Prog. Ser.* 37, 259-264.
- Bethke, C.M., Sanford, R.A., Kirk, M.F., Jin, Q., Flynn. 2011. The thermodynamic ladder in geomicrobiology. *American Journal of Science*. 311, 183 – 210.
- Bruchert, V., Jorgensen, B.B., Neumann, K., Riechmann, D., Schlosser, M., Schulz, H., 2003. Regulation of bacterial sulfate reduction and hydrogen sulfide fluxes in the central namibian coastal upwelling zone. *Geochimica et Cosmochimica Acta.*, 67(23), 4505-4518.
- Chen, M., Walshe, G., Chi Fru, E., Ciborowski, J.H., Weisener, C.G. 2013. Microcosm assessment of the biogeochemical development of sulfur and oxygen in oil sands fluid fine tailings. *App. Geochem.*, 37, 1 – 11.
- Chi Fru, E., Chen, M., Walshe, G., Penner, T., Weisener, C.G. 2013. Bioreactor studies predict whole microbial population dynamics in oil sands tailings ponds. *Applied Microb. and Biotechnol.*, 97(7), 3215 – 3224.
- Elberling, B., Damgaard, L.B., 2001. Microscale measurements of oxygen diffusion and consumption in subaqueous sulfide tailings. *Geochim. Cosmochim. Acta.*, 65, 1897–1905.
- Forster S., Graf, G. 1992. Continuously measured changes in the redox potential influenced by oxygen penetrating from burrows of *Callinassa subterranean*. *Hydrobiologia*. 235/236, 527 – 532.

- Forster S., Graf, G. 1995. Impact of irrigation on oxygen flux into the sediment: intermittent pumping by *Callianassa subterranean* and 'piston-pumping' by *Lanice conchilega*. *Marine Biol.*, 123, 335 – 346.
- Giblin, A.E., Likens, G.E., White, D., Howarth, R.W. 1990. Sulfur storage and alkalinity generation in New England lake sediments. *Limnol. Oceanogr.*, 35(4), 852 – 869.
- Giles, H., Pilditch, C.A., Nodder, S.D., Zeldis, J.R., Currie, K., 2007. Benthic oxygen fluxes and sediment properties on the northeastern New Zealand continental shelf. *Continental Shelf Research*. 27, 2373-2388.
- Haroon, M.F., Hu, S., Shi, Y., Imelfort, M., Keller, J., Hugenholtz, P., Yuan, Z., Tyson, G.W. 2013. Anaerobic oxidation of methane coupled to nitrate reduction in a novel archaeal lineage. *Nature*. 500(7464), 567 – 70.
- Hofman. P. A. G., De Jong, S. A., Wagenvoort, E. J., Sandee, A. J. J., 1991. Apparent sediment diffusion coefficients for oxygen and oxygen consumption rates measured with microelectrodes and bell jars: application to oxygen budgets in estuarine intertidal sediments (Oosterschelde, SW Netherlands). *Mar. Ecol. Prog. Ser.* 69: 261-272.
- Holowenko, F.M., MacKinnon, M.D., Fedorak, P.M., 2000. Methanogens and sulphate-reducing bacteria in oil sands fine tailings waste. *Can J Microbiol.*, 46(10), 927 – 937.
- Joye, S.B., Boetius A., Orcutt, B.N., Montoya, J.P., Schulz, H.N., Erickson M.J., Lugo, S.K. 2004. The anaerobic oxidation of methane and sulfate reduction in sediments from Gulf of Mexico cold seeps. *Chemical Geology*, 205, 219 – 238.
- Knittel, K., Boetius, A. 2009. Anaerobic oxidation of methane: progress with an unknown process. *Annu Rev Microbiol.*, 63, 311 – 34.
- Kuwabara, J.S., van Geen, A., McCorkle, D.C., and Bernhard, J.M., 1999. Dissolved sulphide distributions in the water column and sediment pore waters of Santa Barbara Basin. *Geochimica et Cosmochimica Acta*, v. 63, no. 15, 2199-2209.

- McGinnis, D.F., Berg, P., Brand, A., Lorrai, C., Edmonds, T.J., Wuest, A., 2008. Measurements of eddy correlation oxygen fluxes in shallow freshwaters: Towards routine applications and analysis. *Geophysical Research Letters*. 35, 1-4.
- Melton, E.D., Swanner, E.D., Behrens, S., Schmidt, C., Kappler, A. 2014. The interplay of microbially mediated and abiotic reactions in the biogeochemical Fe cycle. *Nature Reviews Microbiology*. 12, 797 – 808.
- Revsbech, N.P., Nielsen, L.P., Ramsing, N.B., 1998. A novel microsensor for determination of apparent diffusivity in sediments. *Limnol. Oceanogr.* 43, 986-992.
- Revsbech, N.P., Sorensen, J., Blackburn, T.H. 1980. Distribution of oxygen in marine sediments measured with microelectrodes. *Limnol. Oceanogr.* 25(3), 403 – 411.
- Revsbech, N.P. 1989. Diffusion characteristics of microbial communities determined by use of oxygen microsensors. *J. Micro- biol. Meth.*, 9, 111 – 122.
- Richards, S. R., Kelly, C. A. and Rudd, J. W. M., 1991. Organic volatile sulfur in lakes of the Canadian Shield and its loss to the atmosphere. *Limnol. Oceanogr.* **36**, 468-482.
- Sorensen, K., Rehakova, K., Zapomelova, E., Oren, A. 2009. Distribution of benthic phototrophs, sulfate reducers and methanogens in two adjacent saltern evaporation ponds in Eilat, Israel. *Aquatic Microbial Ecology*. 56(2-3), 275-284.
- Siddique, T., Kuznetsov, P., Kuznetsova, A., Arkell, N., Young, R., Li, C., Guidard, S., Underwood, E., Foght J. 2014. Microbially-accelerated consolidation of oil sands tailings. Pathway I: changes in porewater chemistry.
- Siddique, T., Kuznetsov, P., Kuznetsova, A., Li, C., Young, R., Arocena, J.M., Foght J. 2014. Microbially-accelerated consolidation of oil sands tailings. Pathway II: solid phase biogeochemistry. *Frontiers in Microbiology*. 5(107), 1-15.

Thorbergisdottir I.M., Gislason, S.R., Ingvason, H.R., Einarsson, A., 2004. Benthic oxygen flux in highly productive subarctic Lake Myvatn, Iceland: in situ benthic flux chamber study. *Aquatic Ecology*. 38, 177-189.

[In Preparation] VanMensel et al., 2015 – The Proteobacteria response and genomic features of gamma-irradiated oil sands fluid fine tailings: a community structure perspective.

Voordouw, G. 2013. Interaction of oil sands tailings particles with polymers and microbial cells: First steps toward reclamation to soil. *Biopolymers*, 99(4), 257 – 262.

CHAPTER 3:

CRITICAL SHEAR STRENGTH AND BIOSTABILIZATION EFFECTS ON INDUSTRIAL TAILINGS MATERIAL

3.1 Introduction

A GUST microcosm system was used to assess the hydrodynamic shear properties of two different FFT source materials from Suncor Energy Inc. The critical shear strength, describing the point in which complete bed failure occurs, is determined in FFT from both Pond STP (STP) and Pond 1A (P1A). These observations will determine how the shear strength of each FFT product is a function of age and biotic and abiotic characteristics. This biotic vs. abiotic study will determine the effects of biofilm on increasing the critical shear strength of each FFT product. DNA extracted from collected sub samples during the experiment, will indicate how microbial communities affect biofilm formation and structure between FFT sources.

Several studies in recent years have observed the effects of biostabilization on both freshwater and marine sediments subjected to various shearing forces, noting the cohesive effects of microbial biofilms (e.g. de Boer, 1981; Grant, 1988; Noffke, 1998; Noffke and Krumbein, 1999; Friend et al., 2008). Such studies have varied from tidal flats, to inland streams and rivers, to large lakes and marine environments (e.g. Cuadrado et al., 2011; Stone et al., 2011), and are important in determining the likelihood of contaminant transport, such as heavy metals that are

potentially toxic when concentrated (e.g. Azetsu-Scott et al., 2007). However, the biostabilization of particles is not the only governing factor controlling the cohesiveness of sediments. Consolidation (Droppo and Amos, 2001), dewatering (Tolhurst et al., 2000) and electromagnetic interactions (Mehta, 1989) between particles also play a role on the erodibility of sediments, causing cohesiveness between particulates using several mechanisms. Erosion of such particles only occurs once the critical shear strength of the sediment is surpassed by an external hydrodynamic or biological force (e.g. currents, tides, movement of organisms), greater than this critical shear value. Once this threshold is overtaken, resuspension occurs and erosion and transportation of sediments occurs before the suspended solids can settle out again.

The stability of such sediments, caused by biofilm formation, is a result of the attachment of the microbial cells to particulate surfaces through a matrix comprised of extracellular polymeric substances (Donlan, 2002). Variability of these EPS matrices are attributed to the substrate itself, the species of microbial organism and medium in which it grows (e.g. Donlan, 2002; Donlan et al., 1994; Fletcher, 1988). Variations in microbial community structure, as observed in several other studies, proves interesting as specific microbial species can be responsible for measured increases or decreases in critical shear strength, due to variation of the biofilm structure (e.g. Droppo and Amos, 2001; Droppo et al. 1997; Patterson, 1997).

Studying the biostabilization of FFT from oil sands tailings ponds allows for a deeper understanding of the correlation between both the biological and physical characteristics of these ponds, and their corresponding interactions. This research

will observe the effect that biostabilization has on the stability of these systems, limiting resuspension at the FFT-OSPW interface, in order for the cap water to be recycled, and maintain consistent consolidation of the FFT. Cohesive bonding of particles due to biofilms has been shown in other systems to limit erosion rates, therefore potentially limiting the resuspension of not only clays and sands, but also precipitated metals. Investigating the microbial community within each treatment can be used to define roles of specific classes of microorganisms in the stability and structure of these respective FFT products can be observed.

3.2 Methods

3.2.1 Experimental Design – GUST Microcosm

The critical sediment shear strength of two tailings pond FFT material (STP and P1A) was determined using the procedures and methods outlined in the UMCES-Gust Erosion Microcosm System (U-GEMS manual) (Version 1.4; Jan. 2012; SES Consulting). The U-GEMS system measured the erodibility of two sediment cores simultaneously, using a range of shear forces ranging from as low as 0.005 Pa to 0.7 Pa in this study. A nearly uniform shear force was applied to the sediment interface through means of a rotating disk and central suction (Figure 3.1). The desired shear stress is input via computer interface, and pre-calibrated turbidimeter (Hach 2100N turbidimeter) data and motor speeds are recorded using Water2Web software (Green Eyes, LLC) to determine the FFT specific shear strength (see Figure 3.2). Oil sands processed water (OSPW) from the respective tailings ponds from which the FFT samples were obtained, are used as the replacement water source.

The raw turbidimeter data was measured in Nephelometric Turbidity Units (NTU), pre-calibrated for accuracy. Subsamples taken throughout the range of shear stresses were taken to measure TSS based on the NTU measurements. Results of turbidity and correlated shear stress are plotted with respect to time in order to observe particle resuspension/turbidity increase as a function of shear stress and elapsed time.

3.2.2. Fluid Fine Tailings Microcosm/Core set-up

A 2x2 factorial designed microcosm setup was used to distinguish the effects of biostabilization between both fresh (STP) and mature (P1A) tailings materials (table 3.1). Samples were taken from the FFT-OSPW interface of both P1A and STP at the Suncor Energy Inc. operation near Fort McMurray, Alberta, Canada. Stored in 20L sealed buckets, the FFT and OSPW samples were shipped at 4°C, then stored at the same temperature until the initiation of the experiment. Further, the FFT was divided into both biotic and abiotic (sterilized) sediment cores, such that the effects of biofilm vs no biofilm on the stabilization of the FFT can be observed. The samples sterilized for the abiotic systems were sent to the McMaster Institute of Applied Radiation Services (McIARS) in Hamilton, Ontario, Canada. The samples were gamma irradiated for 24 hrs at 28 kGy (Chen et al. 2013) to eliminate any living microbial populations. FFT was poured into each sediment core such the FFT-water interface was 10cm below the top of the core (Figure 3.3), as described in the U-GEMS manual, for proper calibration of applied shear. FFT therefore comprised approximately half of the core volume. The remaining volume was filled with the

respective OSPW from each pond. The sediment cores have a moveable base/plunger with an o-ring to allow for adjustment of the interface level given the likelihood for FFT consolidation. The cores were then capped until the erosion experiments were initiated to inhibit contamination and disruption.

3.2.3 Experimental Procedure

3.2.3.1 GUST Chamber

Outlined in the U-GEMS manual (see 3.2.1) sediment cores are prepared for the erosion events by securing the rotating head and corresponding water lines to the pump, turbidimeters and water source. The experiment is initiated with a 10 minute run at the lowest shear stress setting (0.005Pa) to clear the water cap. The shear stress is then increased at user-defined increments using the Water2Web software (Green Eyes, 2010), starting at 0.01 Pa incrementally increasing applied shear stress until bed failure occurs (see Table 3.2). Each shear stress is held for 5 minutes to allow turbidity to decrease before increasing to the following shear stress. At each shear step, 20ml samples are taken to calibrate suspended solids content (SSC) (mg L^{-1}) with the NTU measured, with the remaining effluent collected for calculations of cumulative eroded mass (CEM) calculations. Both SSC and CEM sub-samples are vacuum-filtered using 47 mm diameter, 0.45um nylon membrane filters. Filtered water volume (ml) and wet/dry weight of the filter are recorded to determine weight of filtered solids (mg) with respect to measured NTU. The mass of filtered samples are cumulated and compared to the shear at which resuspension occurred, in order to obtain CEM measurements.

3.2.3.2 DNA Expression

To determine variation in the biofilms of each pond, and at finite depths within the upper eroded layers of the FFT, subsamples were taken at 4 shear stresses during the erosion experiments. This sample strategy collected biofilm samples from the FFT-water interface then at 3 slightly increasing depths beyond this interface, as erosion progressed. Samples were collected in sterilized 50ml centrifuge tubes and immediately flash-frozen in liquid nitrogen. All samples were then stored at -80°C until DNA extraction.

DNA was extracted from the collected samples using the MOBIO Power Soil DNA Extraction Kit (MOBIO Laboratories, Carlsbad, CA, USA). These methods were preceded with 3 purification steps to remove inhibitors (humic substances and residual bitumen). Specifically, samples were centrifuged at 3500 rpm for 20 minutes to concentrate cells into a pellet, subsequently discarding the supernatant. The pellet was then resuspended in sterilized, deionized water and centrifuged, to clean the sample of inhibitors and residual bitumen. The centrifugation and resuspension was repeated 3 times for improved purification. Approximately 0.5g of sample was then placed in the MOBIO bead tubes, from which the manufacturer prescribed extraction protocol was followed. Completed DNA extractions were then stored at -20°C until samples were analysed. Ion Torrent sequencing was used to sequence and amplify bacterial 16S rRNA genes, from which processed samples were classified using the RDP Pyrosequencing pipeline (<http://pyro.cme.msu.edu>).

3.3. Results and Discussion

3.3.1. *GUST Microcosm Shear Strength*

All turbidity measurements and reference to resuspension causing increase in turbidity are in Nephelometric Turbidity Units (NTU). This is due to variability obtained in calibration to suspended solids content (SSC) through a series of filtered subsamples. Since NTU is directly analogous to SSC based on several tested calibrations, this does not pose a problem for observed results of critical shear strengths and resuspension observations.

The turbidity recorded during the initial erosion experiment (21 days of settling) varied greatly between biotic and abiotic FFT for both pond materials. Figures 3.4 – 3.7 express the turbidity of each system with respect to applied shear stress over the course of the experimental time period. It was apparent very quickly the cohesive effects that the biofilm had on the stabilization of the FFT within both P1A and STP. With respect to the more juvenile abiotic STP (Figures 3.4 and 3.5), it was observed that at applied shear stresses of as low as 0.03 Pa, resuspension of finer particles was already taking place. Further, complete bed failure was evident at only 0.06 Pa, where the turbidity of the system rose significantly as shear further increased to 0.1 Pa, quickly surpassing a turbidity of 1400 NTU (significant quantity of suspended solids observed). On the other hand, the biotic STP FFT was much different. Slight resuspension of lighter/finer particles was observed at approximately 0.08 Pa, but only reached a turbidity of 400 NTU at a shear stress of 0.15 Pa. Thus the amount of sediment eroded in the biotic system was 71.4% lower than that of the abiotic system when subjected to equivalent shear force.

Analyzing the results from the mature Pond 1A (Figures 3.6 and 3.7) further corroborated the biostabilization results found in Pond STP. In this system, the abiotic FFT again eroded at much lower applied shear stress than the biotic system. At 0.15 Pa, the turbidity of the abiotic P1A FFT column began to increase, indicating the initial stages of erosion. Once the shear stress was increased to 0.6 Pa, bed failure had occurred, and the turbidity reached approximately 500 NTU. In relation to the biotic FFT, we observed lower levels of resuspension. Here, at a shear stress of 0.15 Pa, we again observe very slight resuspension, but by 0.6 Pa, turbidity only increases to approximately 300 NTU. In comparison, this is approximately 200 NTU lower than the abiotic system, indicating that the biofilm plays a role in stabilizing the FFT in the mature P1A as well. Furthermore, during the erosion experiments, visual disruption of the biofilm at the FFT-water interface was observed. At moderate shear levels in P1A, the interface would appear to split, peel and roll onto itself. This obviously showed the cohesive nature of the biofilm matrix at the FFT-OSPW interface. However, another interesting observation revolves around the nature of the two pond materials themselves. STP FFT is high in water content, while the mature P1A is more consolidated. These physical variations are why P1A turbidities (both biotic and abiotic) are far lower than those measured in both STP FFTs (abiotic and biotic). This variation between ponds, in terms of overall stability at increasing shear stresses, is likely due to do with time of consolidation and age of each pond rather than the bacteria influence alone. This correlates with previous work done (e.g. Stone et al., 2008; Stone et al., 2011), examining the effects of consolidation on the erodibility of sediments subjected to varying settling times. In

these studies, there is a clear stabilization increase when consolidation time increases, which corresponds to the aged nature of P1A over the freshly processed STP material.

The second simulated erosion experiment was done 21 days following the first (total of 42 days since initiation of experiment) to determine critical shear strength post-disturbance and after re-establishment of the microbial biofilm. This erosion would be done on the same GUST FFT columns as the initial erosion, thus the eroded FFT would consist of the particles beneath the SFGL and uppermost sediment eroded at 21 days. This second erosion would allow changes to the microbial community structure following the initial disturbance to be identified. STP was observed to have considerable consolidation during this time period, particularly in the biotic system, though the abiotic was not too far behind. When subjected to the shear forces in the GUST microcosm, there was still clear variation between the biotic and abiotic STP FFT systems (Figures 3.8 and 3.9). The abiotic STP FFT began to show significant resuspension at approximately 0.08 Pa, with turbidity rising past 90 NTU, quickly spiking to 300 NTU once the shear stress reached 0.25 Pa, indicative of complete bed failure. The biotic STP FFT on the other hand appeared to be more stabilized, with no increase in turbidity until 0.2 Pa, where the turbidity only reached 91 NTU. Bed failure finally occurred once the shear stress was increased to 0.5 Pa, with turbidity reaching 350 NTU. These observations suggest that even after an additional 21 days on consolidation time, STP was still experiencing the effects of biostabilization despite this further consolidation. In fact, in comparing the biotic and abiotic systems of STP, it the

biotic system was still 50% more stable than the sterilized based on the time of bed failure.

In observing results for P1A (Figure 3.10 and 3.11) for the second erosion simulation, it was apparent that the characteristics observed were unlike those of the first erosion. This time, it appeared as though there was no appreciable difference in the FFT critical shear strength between the biotic and abiotic systems. Both behaved quite similar with respect to resuspension of particles, with measured turbidity values reaching approximately 300 NTU at 0.5 – 0.7 Pa in both cases (representing bed failure). Here we expect that the increased time allowed for settling allowed the abiotic system to gain stability due to dewatering and overall consolidation of fine particles, despite the fact that in Chapter 2, little settling was observed in P1A. However, there is also the possibility that the abiotic (sterile) P1A core became contaminated following the first erosion thus began forming a biofilm, leading to a biostabilization effect during the second erosion experiment. No visible indicator or contamination was observed (i.e. geochemical coloration indicating FeS mineralization (Chen et al., 2013), and no DNA could successfully be extracted from these samples, so no conclusive reasoning can be suggested.

The measurements of critical shear strength for each microcosm and pond material are compiled in table 3.3, and are compared to values published for various natural systems. However, it should be noted that the reference studies utilize alternative, in-situ methods to determine critical shear strength, thus could lead to variations between measurements in the GUST system. Further, when comparing to various natural systems, it is obvious that the critical shear strength of the P1A

material is quite high in relation to many studied natural environments. Other systems including rivers and streams, tidal flats etc. have critical shear strengths much lower, ranging from 0.01 Pa (in sterilized freshwater sediments) to 0.07 Pa (biotic freshwater sediments) (Droppo et al., 2007), but increase to >0.21 Pa in some rivers and streams (Stone et al., 2008).

3.3.2. Cumulative Eroded Mass

Further comparison of erodibility characteristics between ponds and between biotic and abiotic FFT was interpreted through cumulative eroded mass as seen in Figures 3.12 and 3.13. Here the breakdown of the mass of eroded material can be observed with respect to ranges of applied shear stress. This allows for the observation of mass eroded due to specific intervals of shear stress. Similar in both P1A and STP, a considerably higher amount of FFT was eroded from the abiotic systems than the biotic systems (50% and 66% respectively). Here the effects of biostabilization are readily apparent. Observing these plots with respect to applied shear stress, it is also observed that the majority of eroded mass is a result of higher shear stresses on the FFT, which is to be expected. Initially, at lower shear stresses, only the finer/lighter particles are eroded and the SFGL. However as the applied shear stress is increased, more and more particles become resuspended, which include heavier sand particles, thus leading to increased eroded mass. Furthermore, comparing P1A to STP, it is apparent that STP erodes with very little applied force comparatively (though is perhaps similar to natural systems). In both the biotic and abiotic STP microcosms, the most eroded mass was recorded under shear of 0.06 –

0.1 Pa (0.38 kg m⁻² for abiotic; 0.1 kg m⁻² for biotic), equating to more than half the total mass eroded. On the other hand, P1A had the majority of its eroded mass occur in the shear of 0.26 – 0.7 Pa (~0.32 kg m⁻² for abiotic; ~ kg m⁻² for biotic), also equating to approximately 50% of the total mass eroded. This comparison indicates the effects of consolidation on the shear strength of the sediment. P1A is an aged pond, therefore the FFT has had a considerable amount of time to settle and dewater, and thus leading to increased resistance to resuspension. STP on the other hand is consistent of freshly processed FFT, characterized by a very high wt. % water, therefore is much more likely to be resuspended, as indicated by these results.

3.3.3. Microbial Community Structure

Sub-samples taken during the erosion experiments for molecular analysis were combined to get a bulk analysis of the microbial community within each pond. The 4 turbid subsamples obtained from the effluent of the GUST chamber during each experiment (as explained in 3.2.3.2) contained too little volume of sediment/cells to extract any quantifiable quantities of DNA, therefore all samples (i.e. all samples representing defined layers of sediment) were compiled for this analysis, in order to gain a useable yield of extracted DNA. Furthermore the nature of these tailings samples is such that a 3-step washing with sterilized deionized water was needed to remove inhibitors and residual bitumen to obtain *purified* DNA. Thus, in comparing P1A to STP with respect to their microbial phylums (Figure 3.14), it becomes apparent that P1A contains a higher proportion of

Bacteroidetes and *Euryarchaeota*, and a lower proportion of *Proteobacteria* with respect to STP. This indicates that P1A has progressed towards a methane producing stage, while STP largely consists of active SRB communities. Furthermore, observing the classes of *Proteobacteria* within each of the FFT materials (Figure 3.15), additional variation is evident. P1A contains a higher proportion of *Gammaproteobacteria* at 13%, indicating a more diverse microbial population consisting of aerobic and/or facultative bacteria, highly diverse in their degradation capabilities. This correlates to the mature nature of P1A, where the microbial community has had time to grow and adapt. STP on the other hand contains only 2% *Gammaproteobacteria*, 1% *Alphaproteobacteria*, and is almost entirely dominated by *Betaproteobacteria* (97%). Relating to the physical characteristics of these FFT materials, this microbial community variation could also be a result of the aforementioned consolidated vs. freshly processed nature of P1A and STP respectively. The consolidated nature of P1A is perhaps a more viable substrate for which microbes to establish a biofilm between sediment grains, while the liquid nature of STP may pose a hindrance to the establishment of a structured biofilm on solid substrates or at least a weaker biofilm than P1A. Such variation in the mineralogical variation between ponds, and at finite depth intervals within the FFT will be studied in future work, to identify the preferred mineralogical substrate for this biofilm growth. Further, two future, corresponding publications will identify specific similarities and differences between STP and P1A FFT, with respect to the microbial communities in static microcosm systems (VanMensel et al., 2015),

and microbial communities established in simulated erosion experiments on FFT, in the GUST microcosm system (Reid et al., 2015).

3.4. Conclusions

The use of the GUST microcosm to assess the stability of tailings material from the Athabasca Oil Sands is a novel means by which to characterize the resuspension properties of FFT within tailings pond environments. This dynamic microcosm study enables a more accurate means by which to characterize these ponds, simulating natural hydrodynamics causing resuspension of FFT and therefore erosion. In this study we were able to determine the effectiveness of biofilm in stabilizing the FFT early on in the settling process. Initially, there is an obvious biostabilization effect when compared to sterilized, abiotic materials. However, as settling and consolidation proceed, this variation becomes negligible in the aged P1A material, since the abiotic system experienced the same level of stability as the biotic system. This similarity likely due to dewatering and consolidation, but also perhaps due to contamination following the first erosion experiment, though not confirmed by molecular analysis. The fresh tailings of STP however still exhibited a biostabilization effect at the time of the second erosion experiment, contributing to a 50% increase in stability over the sterilized material. Furthermore, in observing cumulative eroded mass calculations, it is again evident that sterilized FFT is resuspended more readily, and in higher quantities at comparable shear stresses compared to biotic FFT. In addition, the younger STP experienced similar quantities of eroded mass though at much lower shear stress

levels. This indicates the easily eroded nature of STP, since it is juvenile tailings with little consolidation to date. These variations between ponds are further emphasized by the molecular results. Microbial community variation between ponds is predominantly observed with respect to *Proteobacteria* proportions. There is clear dominance of this phylum within STP, of which 97% is *Betaproteobacteria*, while P1A is much more diverse, containing >10% *Euryarchaeota*, and twice the *Bacteroidetes* of STP. These observations are to be expected, again due to the variance in age between both pond materials. This definite age difference allowed for the microbial population within P1A to establish and evolve into a diverse and facultative community more-so than STP (VanMensel, 2015). This age variation also played a role in the overall shear strength of the tailings, since the heavily consolidated P1A FFT exhibited a higher stability than STP. However, at this time the details are still unclear how the initial variation in the microbial community structure may have influenced the stability of the FFT, for both STP and P1A.

These results and conclusions support the hypotheses outlined in Chapter 1, indicating that the biotic FFT would exhibit increased stability over the sterilized (abiotic) FFT. Further, the P1A FFT had higher critical shear strength than the STP FFT, further supporting the initial hypotheses. It was not expected, that the critical shear strengths of the aged P1A material in the second erosion event would be nearly identical, though this could be attributed to the aforementioned contamination between erosion experiments, or simply significant dewatering and consolidation.

3.5. Future Work and Improvements

This biostabilization study on FFT from the Athabasca Oil Sands has given great insight into the capabilities of the GUST microcosm system, indicating the possibility for improved experimental design. In attempting to characterize the microbial community structure at finite layers within the eroded sediment, it was determined that sample size played an inhibiting role in the ability to extract useful quantities of quality DNA. Future work on these oil sands tailings materials, as well as other systems, will benefit greatly from increasing subsample sizes and adding several purification steps, in order to obtain measureable yields of *purified* nucleic acids. Furthermore, molecular and microscopic techniques could be employed to identify how specific microbial species influence the stability of the FFT, through variation in integrated biofilm/EPS structures. In addition to that, these tailings ponds can be compared to natural reference lakes sediments from the same geographical location, in order to gain accurate information for use as comparators in computer modeling and simulations. Supplementary density profiles within the FFT could also be implemented to definitively distinguish the microbial role from natural and physical settling/consolidation causing increased shear strength of the FFT.

Figure 3.1: Experimental design of the U-GEMS systems, showing sediment core, motor and erosion head, turbidimeter, pump, sample collection and water flow. (Gust and Muller, 1997)

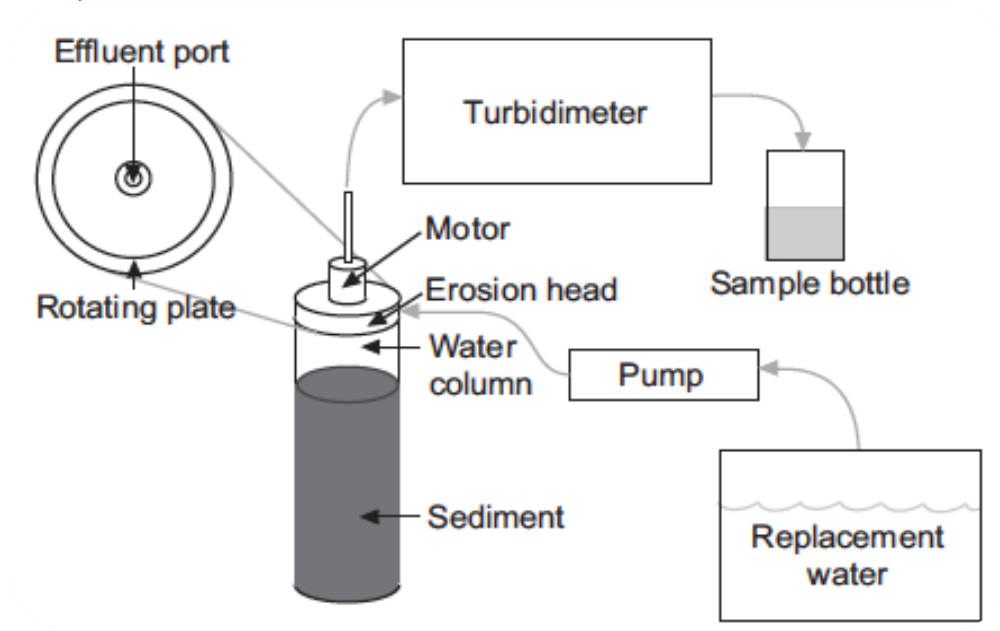


Figure 3.2: Shear strength experimental setup consisting of computer and software, two turbidimeters, pump, calibrated speed control unit, two core samples and rotating disks.

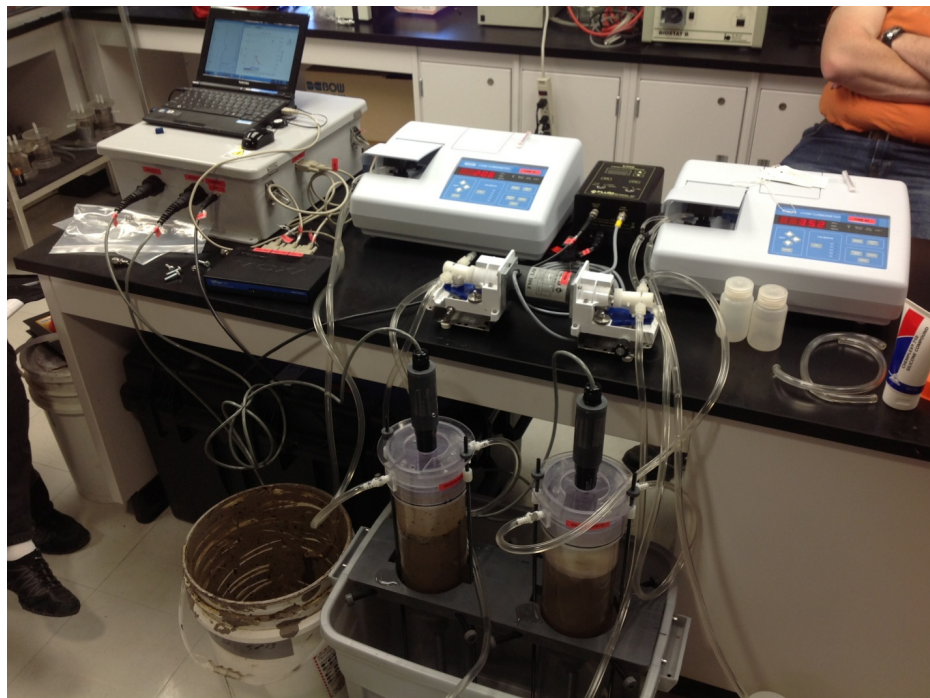


Figure 3.3. GUST microcosm with the 10cm water column between the rotating head and FFT-water interface for proper calibration of shear stress at the interface

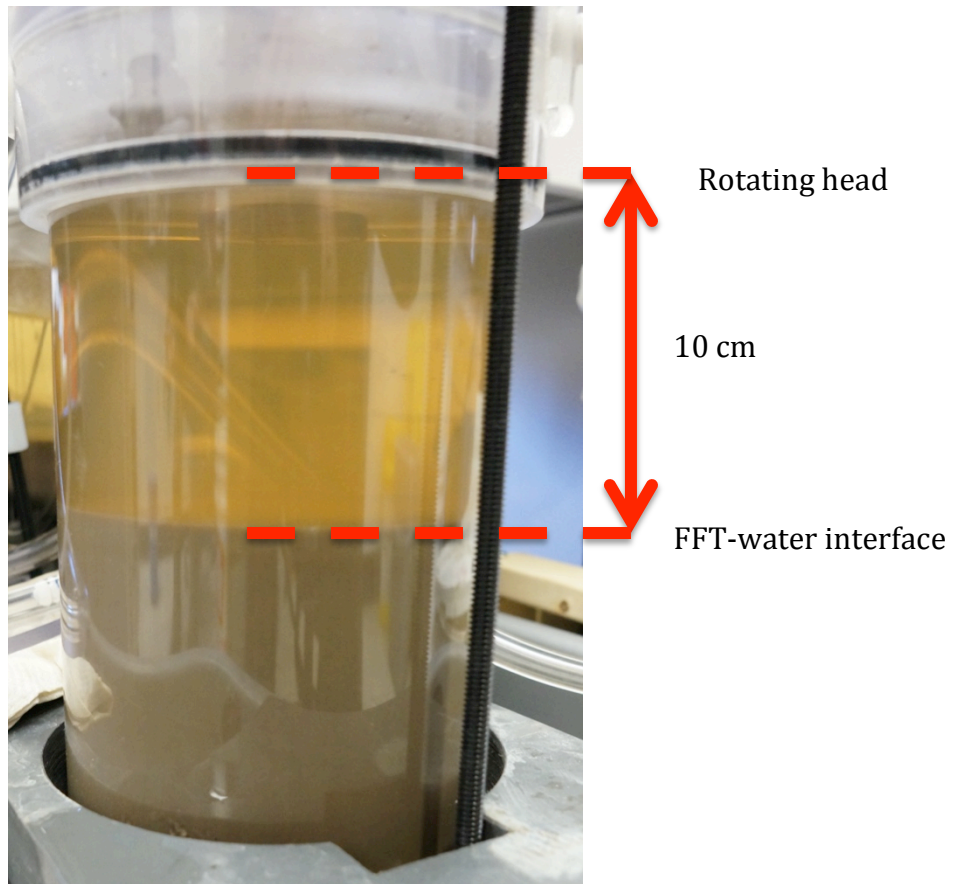


Figure 3.4. Turbidity vs Shear stress plot for **biotic STP** indicating water column turbidity with respect to applied shear force in Gust Microcosm for **first erosion event (21 days)**.

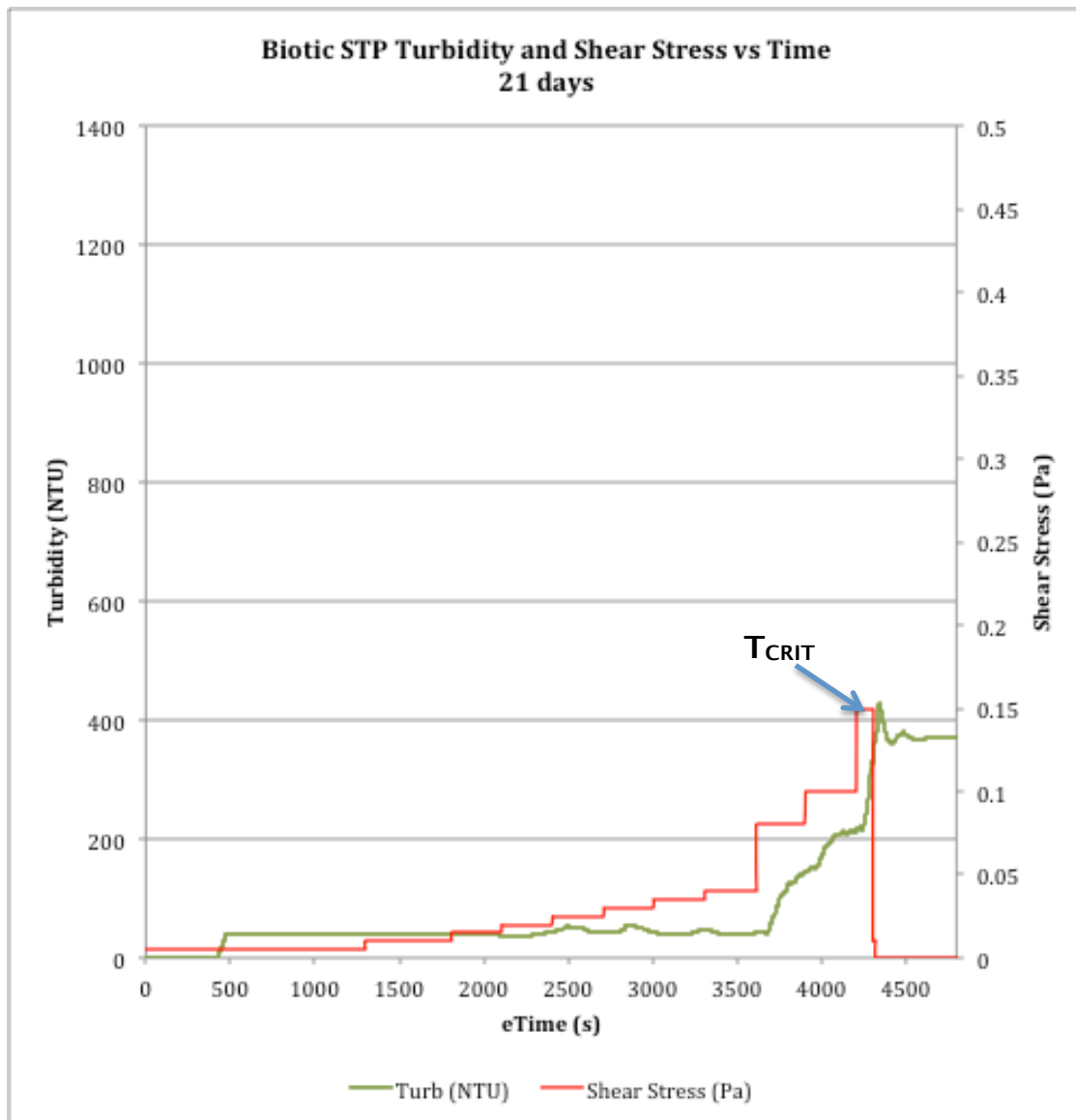


Figure 3.5. Turbidity vs Shear stress plot for **abiotic STP** indicating water column turbidity with respect to applied shear force in Gust Microcosm for **first erosion event (21 days)**.

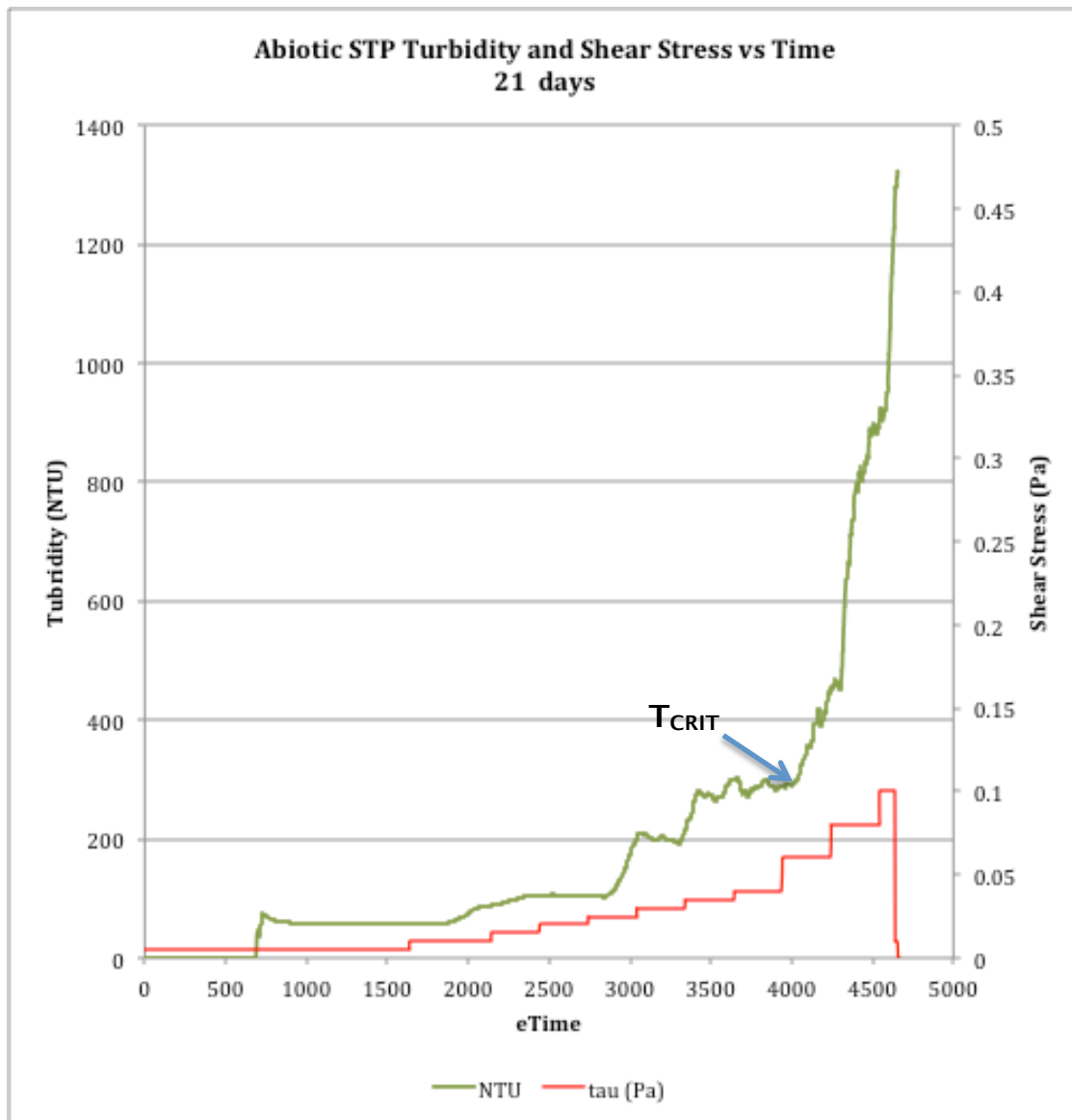


Figure 3.6. Turbidity vs Shear stress plot for **biotic P1A** indicating water column turbidity with respect to applied shear force in Gust Microcosm for **first erosion event (21 days)**.

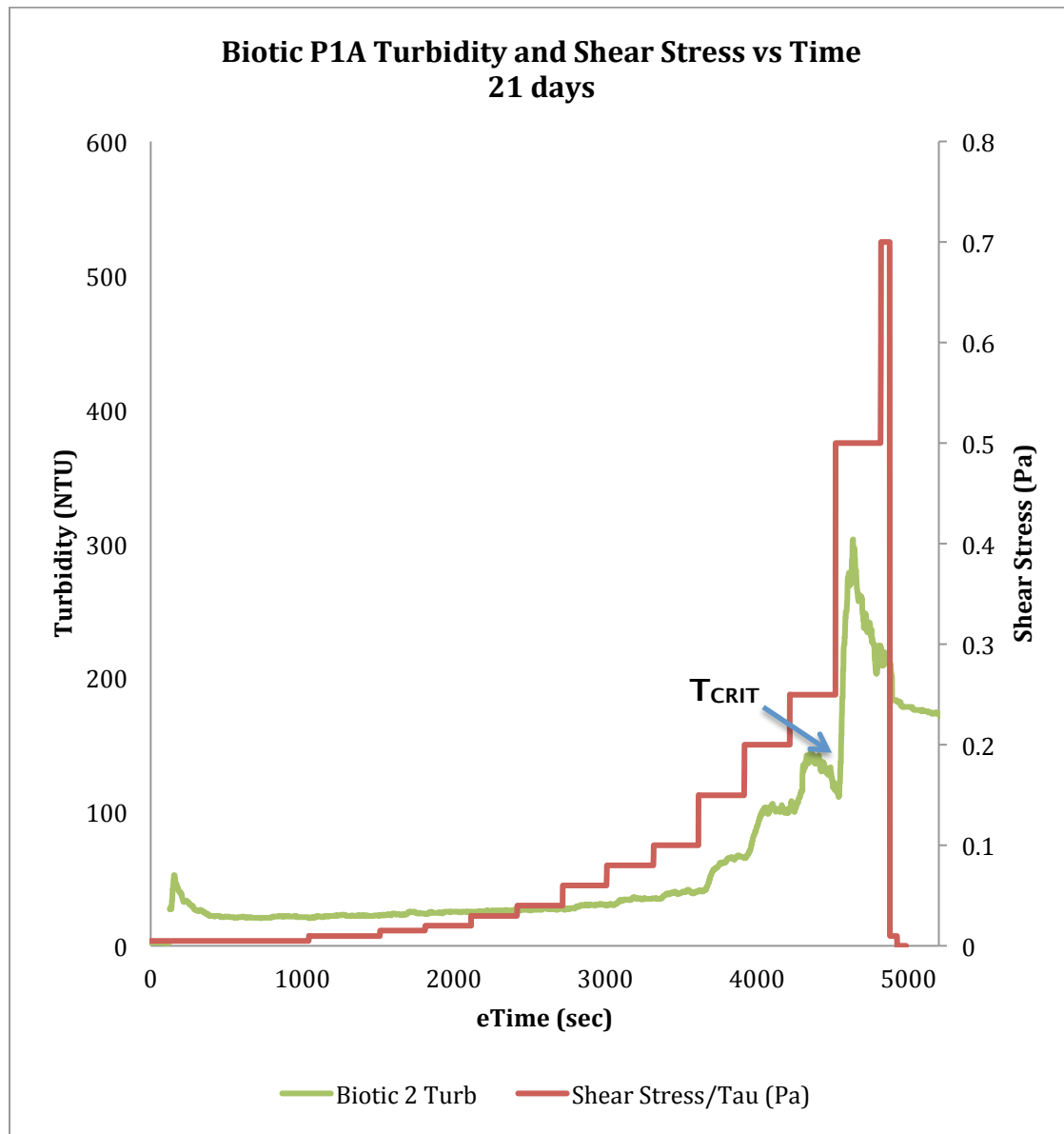


Figure 3.7. Turbidity vs Shear stress plot for **abiotic P1A** indicating water column turbidity with respect to applied shear force in *Gust* Microcosm for **first erosion event (21 days)**.

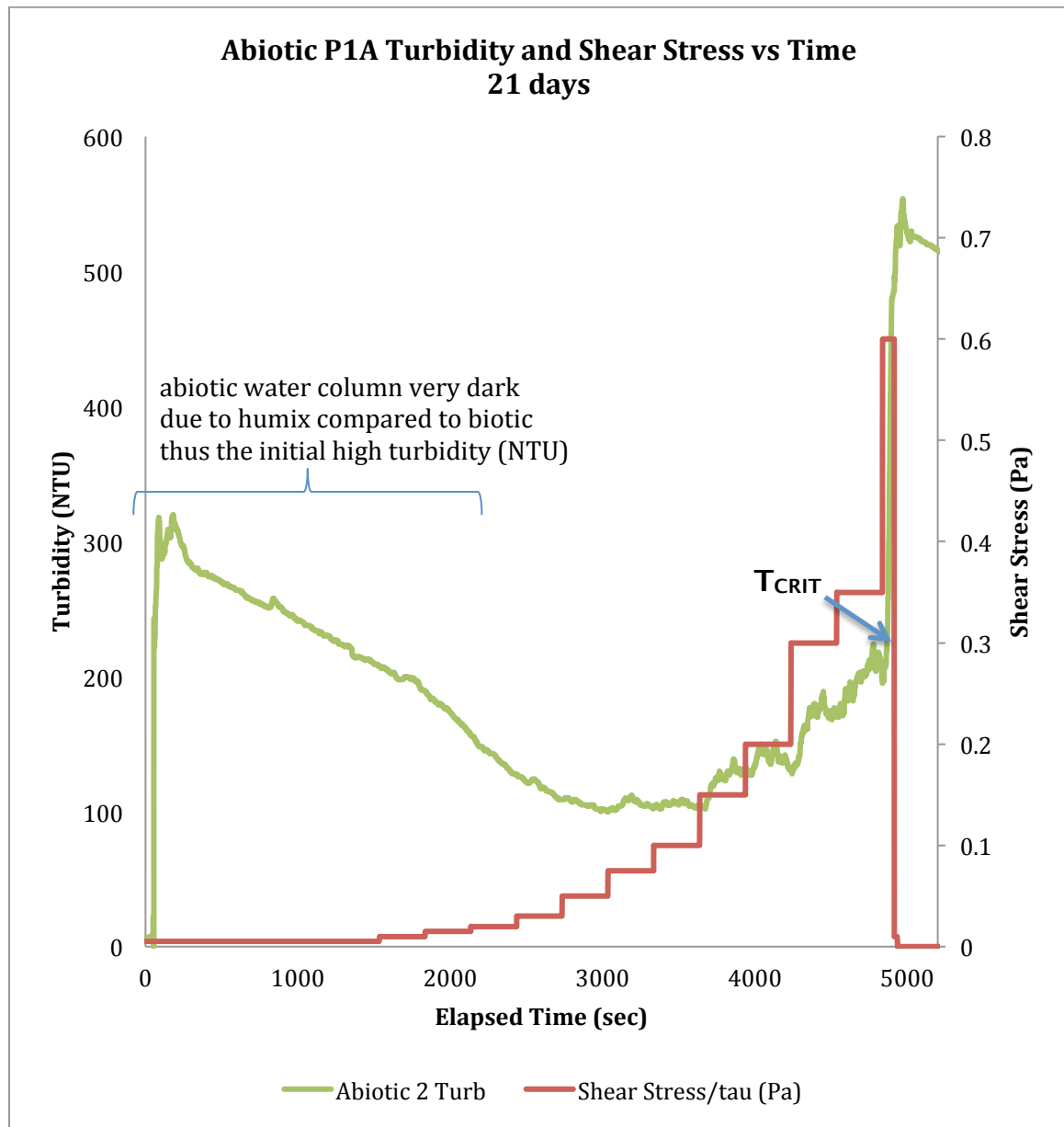


Figure 3.8. Turbidity vs Shear stress plot for **biotic STP** indicating water column turbidity with respect to applied shear force in Gust Microcosm after the **second erosion event (42 days)**.

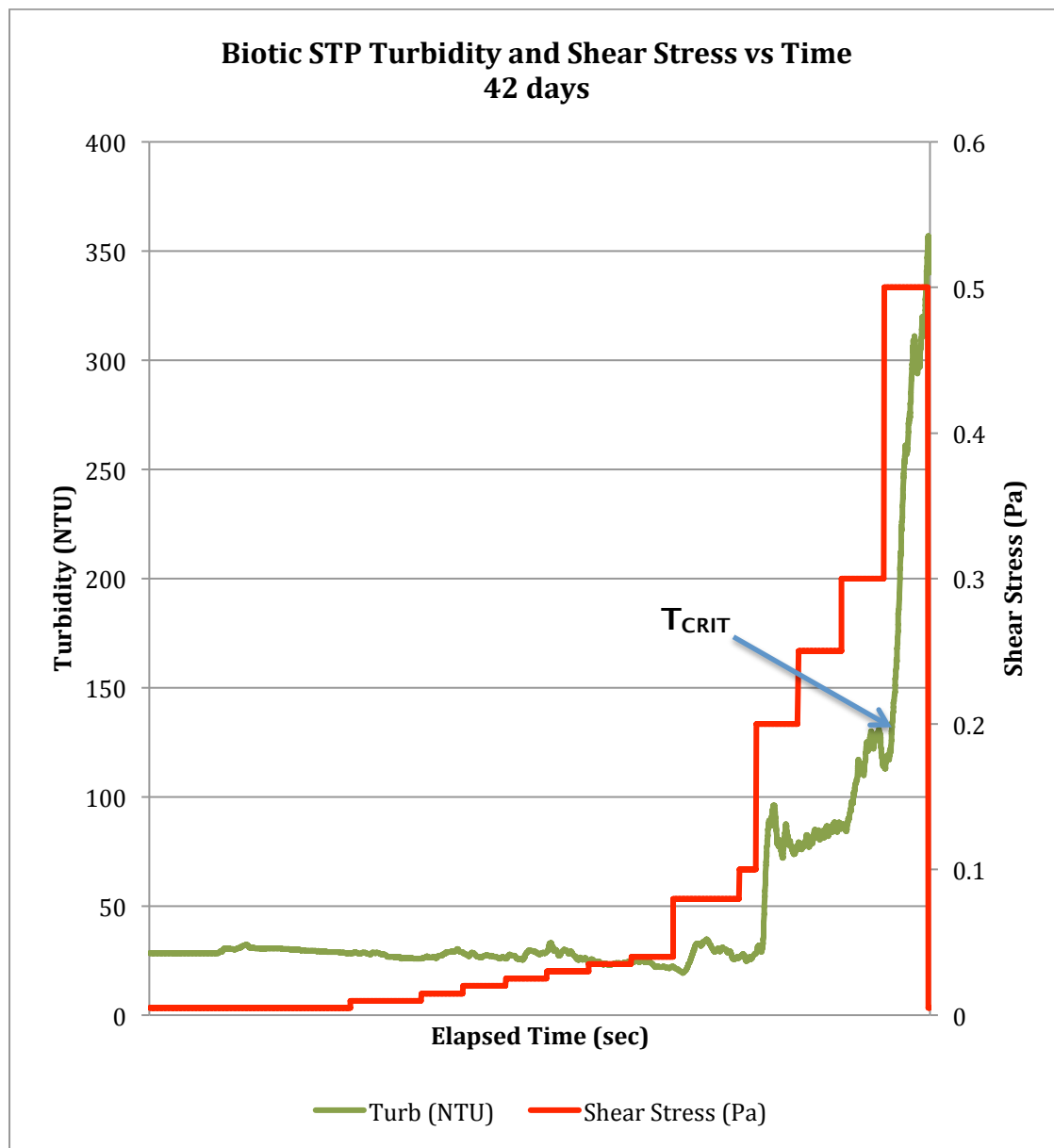


Figure 3.9. Turbidity vs Shear stress plot for **abiotic STP** indicating water column turbidity with respect to applied shear force in Gust Microcosm after the **second erosion event (42 days)**.

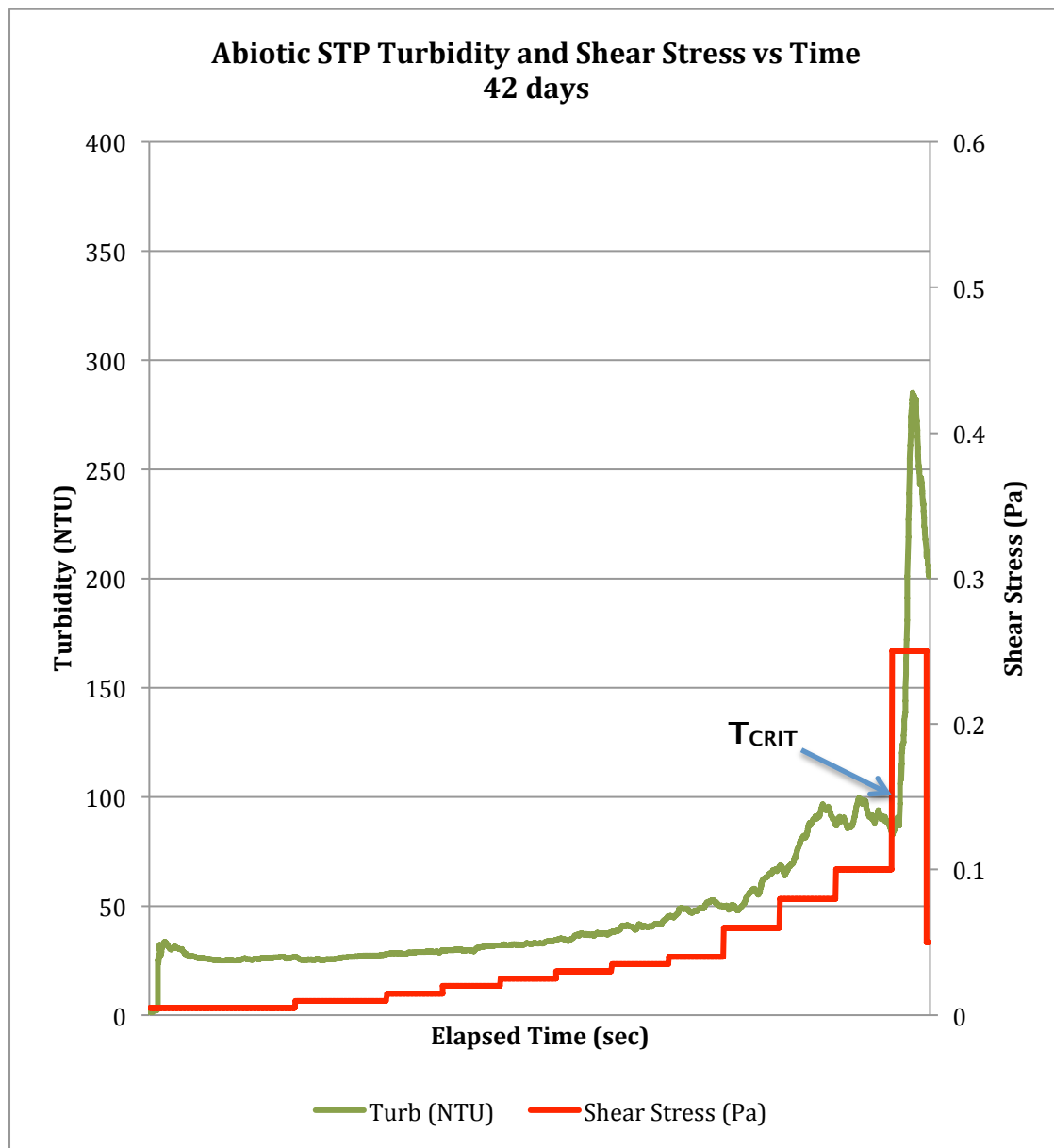


Figure 3.10. Turbidity vs Shear stress plot for **biotic P1A** indicating water column turbidity with respect to applied shear force in Gust Microcosm after the **second erosion event (42 days)**.

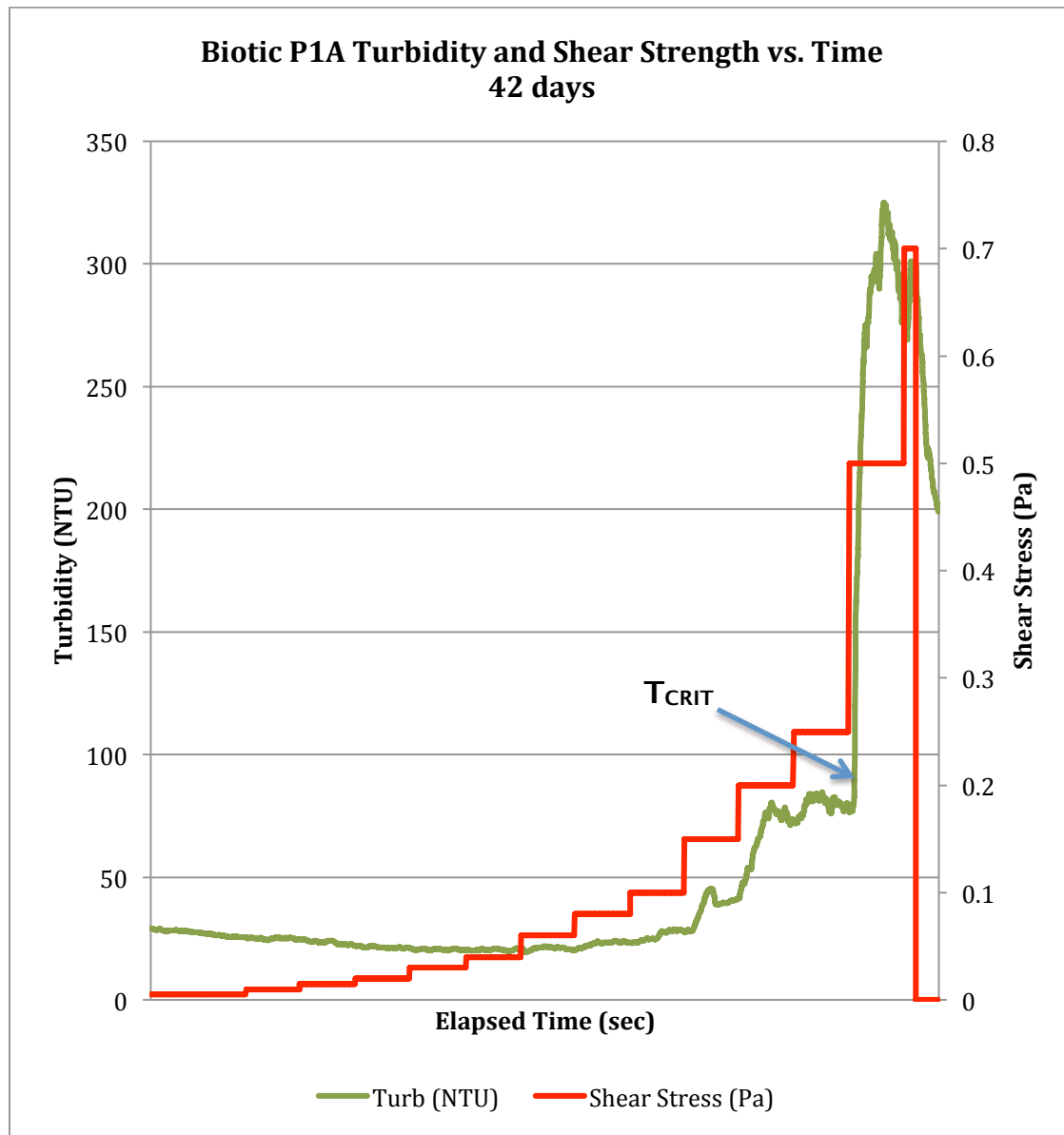


Figure 3.11. Turbidity vs Shear stress plot for **abiotic P1A** indicating water column turbidity with respect to applied shear force in Gust Microcosm after the **second erosion event (42 days)**.

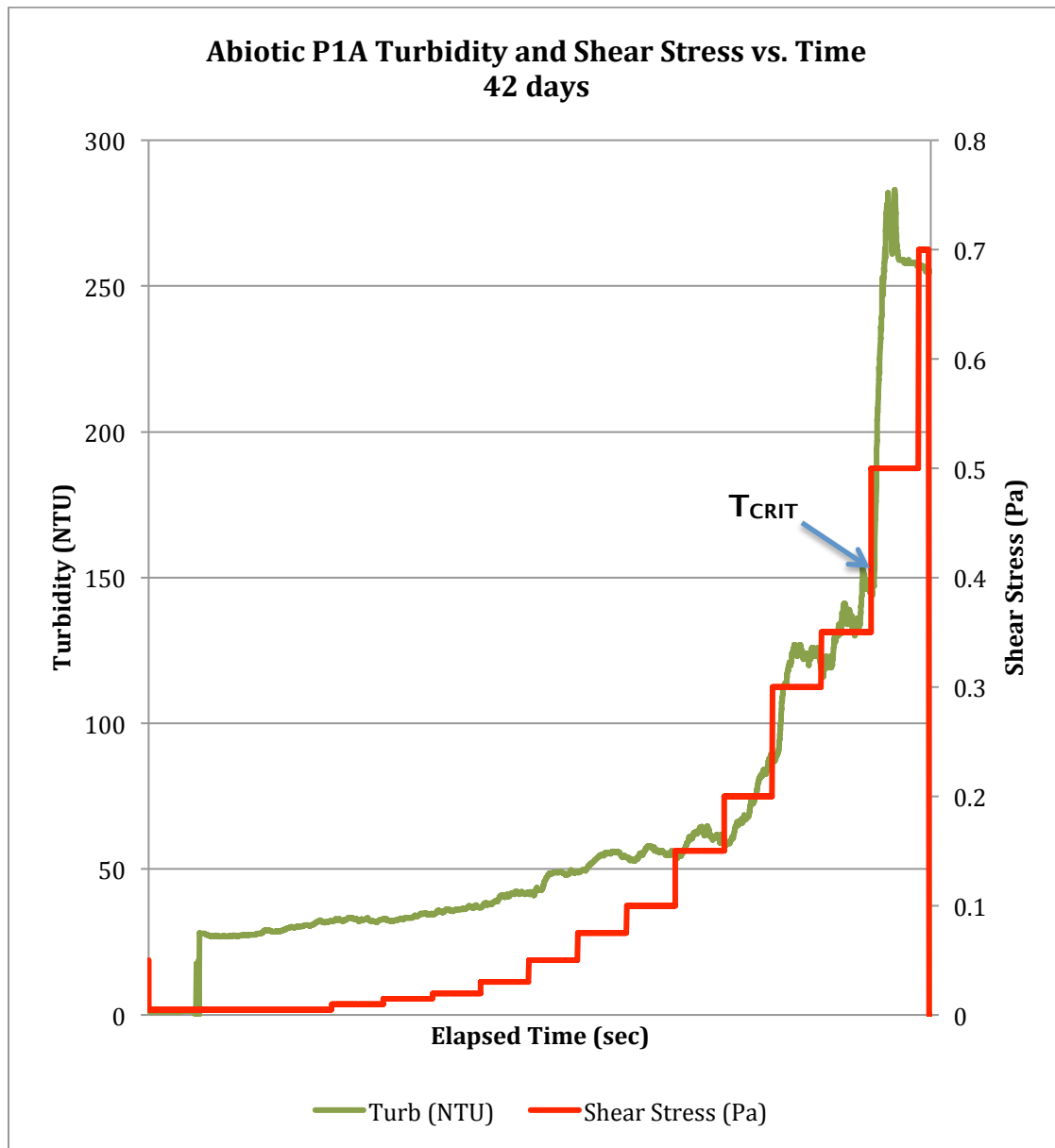


Figure 3.12. Comparison of the cumulative eroded mass between biotic and abiotic P1A during erosion #1 (21 days), indicating the biofilms ability to resist the resuspension of particles even up to relatively high shear stresses.

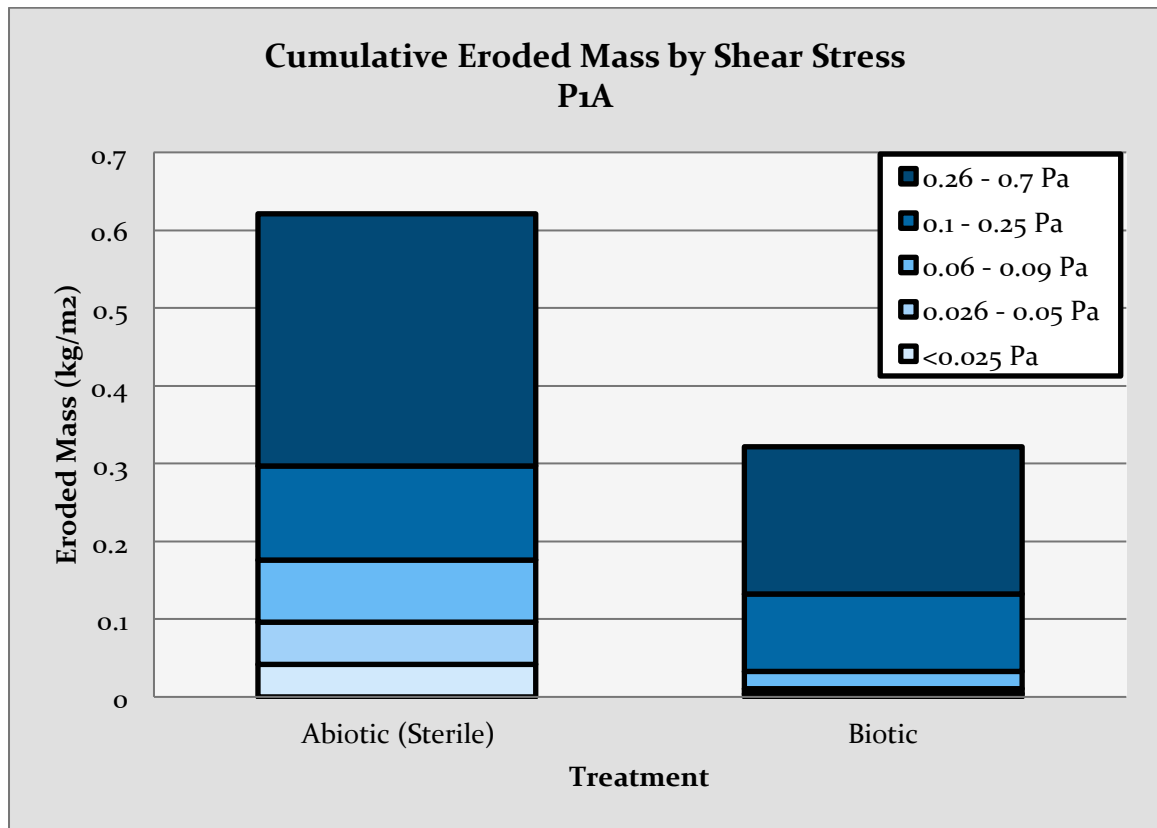


Figure 3.13. Comparison of the cumulative eroded mass between biotic and abiotic STP during erosion #1 (21 days), indicating the biofilm's ability to resist the resuspension of particles even up to relatively high shear stresses. STP also shows high resuspension amounts despite very low applied stress compare to P1A.

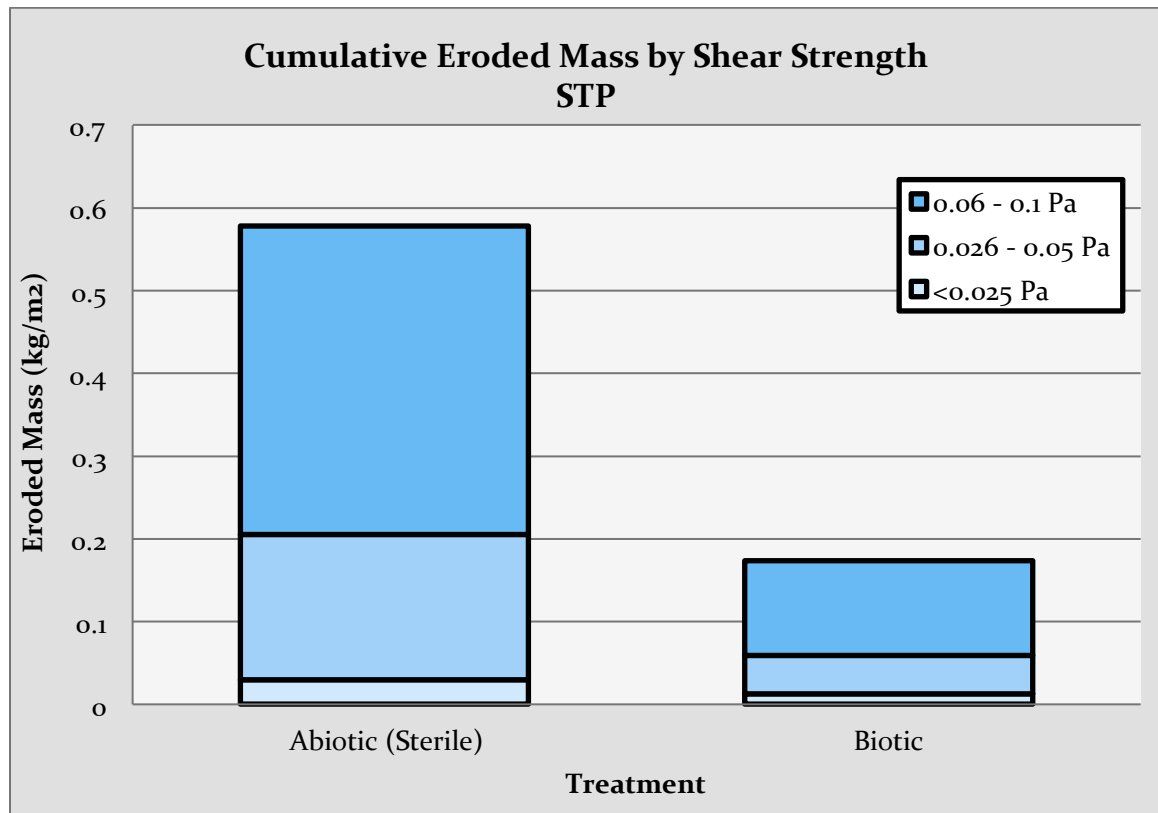


Figure 3.14. Microbial community hierarchy by phylum comparing P1A to STP, indicating a significant difference between the proteobacteria proportions between ponds likely due to the age of each pond.

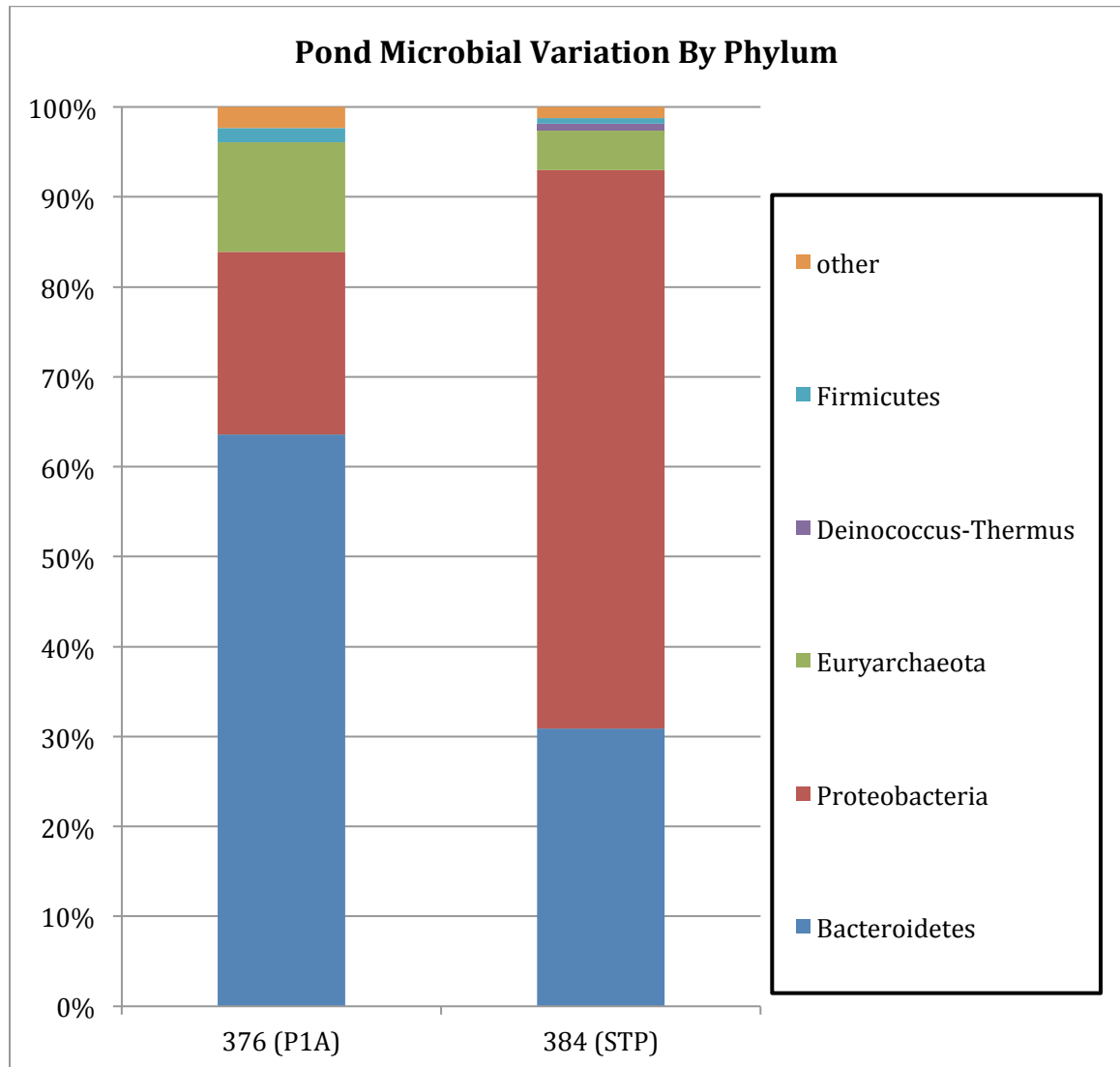


Figure 3.15. Microbial community structure of both P1A and STP with respect to classes of proteobacteria, indicating the higher proportion of gammaproteobacteria in Pond 1A, over the primarily betaproteobacteria dominated Pond STP.

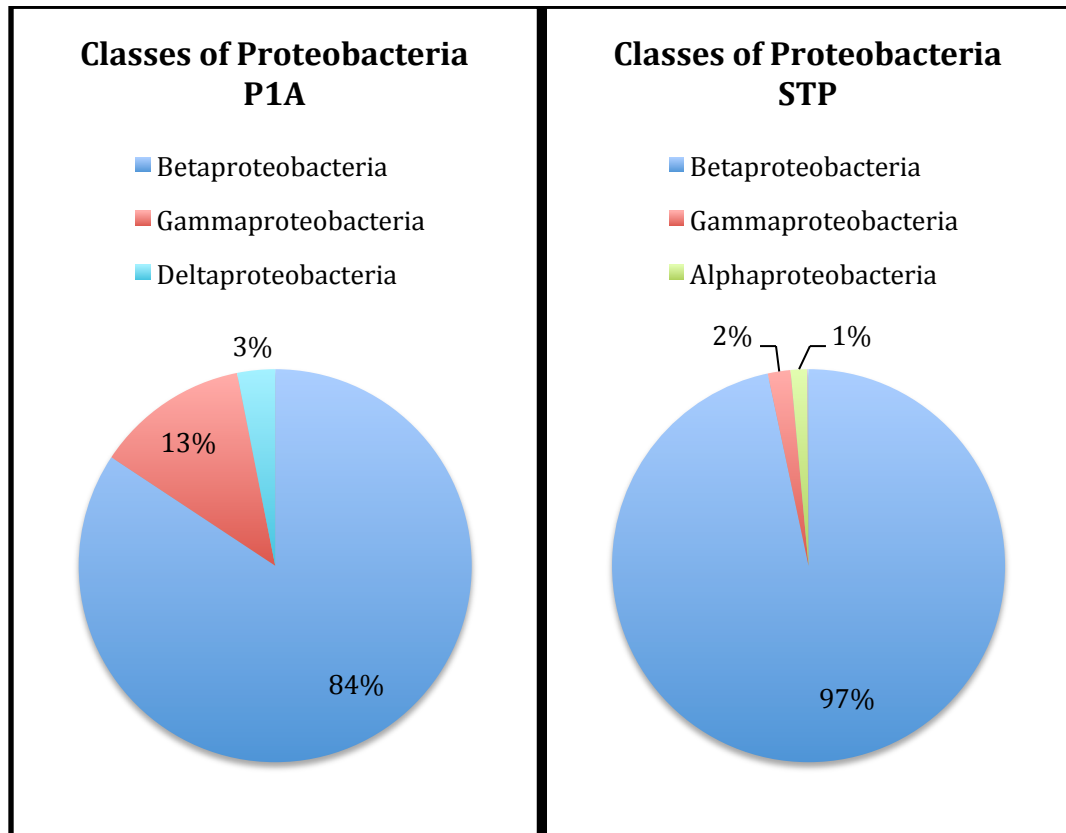


Table 3.1: Microcosm/Core setup for the U-GEMS system. Duplicate cores will be measured for both biotic and abiotic treatments of each of the two sediment types.

Sediment Type/Source:	Treatment:	# of Cores/Microcosms:
Pond 1A (~36 years old)	Biotic	2
	Abiotic	2
Pond STP (Fresh FFT ~8 years old)	Biotic	1*
	Abiotic	1*

**Duplicates were not possible due to insufficient sample volume obtained from tailings pond*

Table 3.2. Series of consecutive applied shear stresses for the respective FFT material used for each erosion experiment; all FFT were run at 0.005 Pa for a 10 minute clearing stage, with each shear stress thereafter for 5 minutes

Erosion Event	FFT Material	Applied Shear Stresses (Pa)
21 days (#1)	Biotic STP	0.005, 0.01, 0.015, 0.02, 0.025, 0.03, 0.035, 0.04, 0.08, 0.1, 0.15
	Abiotic STP	0.005, 0.01, 0.015, 0.02, 0.025, 0.03, 0.035, 0.04, 0.06, 0.08, 0.1
	Biotic P1A	0.005, 0.01, 0.015, 0.02, 0.03, 0.04, 0.06, 0.08, 0.1, 0.15, 0.2, 0.25, 0.5, 0.7
	Abiotic P1A	0.005, 0.01, 0.015, 0.02, 0.03, 0.05, 0.075, 0.1, 0.15, 0.2, 0.3, 0.35, 0.6
42 days (#2)	Biotic STP	0.005, 0.01, 0.015, 0.020, 0.025, 0.03, 0.035, 0.04, 0.08, 0.1, 0.2, 0.25, 0.3, 0.5
	Abiotic STP	0.005, 0.01, 0.015, 0.020, 0.025, 0.03, 0.035, 0.04, 0.06, 0.08, 0.1, 0.25
	Biotic P1A	0.005, 0.01, 0.015, 0.02, 0.03, 0.04, 0.06, 0.08, 0.1, 0.15, 0.2, 0.25, 0.5, 0.7
	Abiotic P1A	0.005, 0.01, 0.015, 0.02, 0.03, 0.05, 0.075, 0.1, 0.15, 0.2, 0.3, 0.35, 0.45, 0.6

Table 3.3. Critical shear strength values for this study compared to several previously published results for natural systems

Study System	Critical Shear Strength (Pa)	
	Biotic	Abiotic
STP (21 days)	> 0.15	0.06
STP (42 days)	0.50	0.25
P1A (21 days)	> 0.70	0.60
P1A (42 days)	0.50	0.50
¹ Kaolinite, Wave-dominated freshwater	0.03-0.07	0.01
² Hay River, NW Territories;	0.21	NA

¹**Droppo et al., 2007**
²**Stone et al., 2008**

3.6. References

- Azetsu-Scott, K., Yeats, P., Wohlgeschaffen, G., Dalziel, J., Niven, S., Lee, K., 2007. Precipitation of heavy metals in produced water: Influence on contaminant transport and toxicity. *Marine Environmental Research*, 63(2), 146 – 167.
- Chen, M., Walshe, G., Chi Fru, E., Ciborowski, J.H., Weisener, C.G. 2013. Microcosm assessment of the biogeochemical development of sulfur and oxygen in oil sands fluid fine tailings. *App. Geochem.*, 37, 1 – 11.
- Cuadrado D.G., Carmona N.B., Bournod C., 2011. Biostabilization of sediments by microbial mats in a temperate siliciclastic tidal flat, Bahia Blanca estuary (Argentina). *Sedimentary Geology*, 237, 95 – 101.
- De Boer, P. L. 1981. Mechanical effects of micro-organisms on intertidal bedform migration. *Sedimentology*, 28, 129- 132.
- Decho A.W., 1990. Microbial exopolymer secretions in ocean environments – their role(s) in food webs and marine processes. *Oceanography and Marine Biology*, 28, 73–153.
- Donlan, R.M., Pipes, W.O., Yohe, T.L. 1994. Biofilm formation on cast iron sub-strata in water distribution systems. *Water Res*, 28, 1497–1503.
- Donlan, R.M. 2002. Biofilms: microbial life on surfaces. *Emerging Infectious Diseases* 8, 881–890.
- Droppo, I.G., Leppard, G.G., Flannigan, D.T., Liss, S.N. 1997. The freshwater flc: A functional relationship of water and organic and inorganic flocc constituents affecting suspended sediment properties. *Wat. Air Soil Pollut.*, 99, 43 – 53.
- Droppo, I.G., Amos, C.L., 2001. Structure, stability and transformation of contaminated lacustrine surface fine-grained laminae. *J. Sediment. Res.* 71, 717 - 726.

- Droppo, I.G., Ross, N., Skafel, M., Liss, S.N. 2007. Biostabilization of cohesive sediment beds in a freshwater wave-dominated environment. *Limnol. Oceanogr.*, 52(2). 577 – 589.
- Flemming, H.C. 2011. The perfect slime. Colloids and Surfaces. *B-Biointerfaces*, 86, 251 – 259.
- Fletcher, M. 1988. The applications of interference reflection microscopy to the study of bacterial adhesion to solid surfaces. In: Houghton D.R., Smith R.N., Eggins H.O.W., editors. *Biodeterioration 7*. London: Elsevier Applied Science; p. 31–50.
- Friend P.L., Lucas C.H., Holligan P.M., Collins M.B., 2008. Microalgal mediation of ripple mobility. *Geobiology*, 6, 70–82
- Grant J., 1988. Intertidal bedforms, sediment transport, and stabilisation by benthic microalgae. P.L. de Boer, A. van Gelder, S.D. Nio (Eds.), *Tide-influenced Sedimentary Environments and Facies*, D. Reidel, Dordrecht, the Netherlands. 499 – 510.
- Grant, J., U. V. Bathmann, and E. L. Mills. 1986. The in-teraction between benthic diatom films and sediment trans-port. *Estuarine, Coastal and Shelf Science*, 23, 225 - 238.
- Green Eyes, L. (2010). U-GEMS Manual Version 1.4.
- Gust, G., Muller, V., 1997. Interfacial hydrodynamics and entrainment functions of currently used erosion devices. Burt, N., Parker, R., Watts, J. (Eds.), *Cohesive Sediments*, Wallingford, UK, 149–174.
- Lévesque, L.M.J. and De Boer, D.H., 2000. Trace element chemistry of surficial fine-grained laminae in the South Saskatchewan River, Canada. *International Association of Hydrological Sciences Publication*, 263, 183-190.
- Mehta, A.J., 1989. On estuarine cohesive sediment suspension behaviour. *J. Geophys. Res.* 94, 14303 - 14314.

- Noffke N., 1998, Multidirectional ripple marks rising from biological and sedimentological processes in modern lower supratidal deposits (Mellum Island, southern North Sea). *Geology*, 26, 879 – 882.
- Noffke N., Krumbein W.E., 1999. A quantitative approach to sedimentary surface structures contoured by the interplay of microbial colonization and physical dynamics. *Sedimentology*, 46, 417 – 426.
- Paterson, D. M. 1997. Biological mediation of sediment erodibility: Ecology and physical dynamics. N. Burt, E. J. Prager, J. G. Southard, and E. R. Vivoni Gallart [eds.], *Cohesive sediments*. Wiley. 215 – 229.
- [In Preparation] Reid, T., Droppo, I., Weisener, C.G.. 2015 – Critical Shear Strength and Biostabilization effects of industrial tailings material (tentative title)
- Stone, M., Krishnappan, B.G., Emelko, M.B. 2008. The effect of bed age and shear stress on the particle morphology of eroded cohesive river sediment in an annular flume. *Water Research*, 42, 4179 – 4187.
- Stone M., Emelko M.B., Droppo I.G., Silins U., 2011. Biostabilization and erodibility of cohesive sediment deposits in wildfire-affected streams. *Water Research*, 45, 521 - 534.
- Tolhurst, T.J., Reithmueller, P., Paterson, D.M., 2000. In situ versus laboratory analysis of sediment stability from intertidal mudflats. *Continental Shelf Res.* 20 (10/11), 1317 - 1334.
- [In Preparation] VanMensel, D., Chaganti, S.R., Boudens, R., Reid, T., Prakasan M.R.S., Ciborowski, J.H., Weisener, C.G. 2015 – The Proteobacteria response and genomic features of gamma-irradiated oil sands fluid fine tailings: a community structure perspective.

CHAPTER 4:

CONCLUSIONS, LIMITATIONS AND FUTURE DIRECTIONS

4.1 Summary and Conclusions

This thesis set out to explain the biogeochemical processes responsible for variations in O_2 and HS^- flux, and methane expression across the FFT-OSPW interface in several FFT products varying in age/maturity. These processes were studied in a static, microcosm-based laboratory study over the course of 52 weeks. Further, the effects of dynamic shearing on the resuspension at the FFT-OSPW interface was studied to deepen our understanding of the physical nature of this interface, when subjected to forces at the interface. These experiments were performed at two different time points (separated by 21 days), to determine both the effects of consolidation/settling and biofilm formation on the stability of FFT. Preliminary molecular analysis was performed to gain insight into how the microbial community varied between ponds and treatments, though proved difficult due to complexity of the sample, and experimental procedures.

Chapter 2 described the static, microcosm-based study using FFT products from both P1A and STP. Definite variation in the diffusive fluxes between STP and P1A were observed, attributed to the physical nature of the FFT, age and microbial community leading to variations in reduced chemical species over time. These results were further compared to WIP (Chen et al. 2013), where all FFT products

were unique from a biogeochemical response perspective (e.g. the flux relationships) but do share obvious similarities with respect to their tendency to form stratified REDOX conditions. Furthermore, observed gas expression proved insightful, lack of methane measured in biotic P1A headspace samples was attributed to the presence of methane oxidizing bacteria. On the other hand, steadily increasing concentrations of methane within the sterile control P1A indicated the likely presence of trapped CH₄ within aged tailings material, also suggested by Voordouw (2013) and Holowenko et al. (2000). These observed variations between biotic and sterilized systems indicates the dominant microbial influence on these FFT materials both early on, as is the case for STP, and later in more mature FFT indicative of P1A. The physico-chemical data and flux measurements recorded during the duration of this study for the two FFT products will contribute to an expanding database which can be applied to both conceptual and numerical models used to predict the behaviors of FFT products used in EPLs and natural wetlands.

Chapter 3 explored a more dynamic experimental study to evaluate the shear strength of both FFT products, and determine how the formation of a biofilm can increase stabilization at the FFT-OSPW interface. In this study, it was determined that biofilm formation in both P1A and STP after 21 days had a definite stability effect when compared to the abiotic control. Furthermore, after 42 days (though utilizing the same FFT source with no further settling of suspended particulates), this biostabilization was still obvious in STP FFT, though became negligible in the

P1A cores. It was suggested that either considerable settling/consolidation, or perhaps even contamination of the microcosm led to this result. Though not visually observed, such contamination would have allowed for biofilm formation, therefore stabilizing the abiotic control to measurements comparable to the biotic P1A FFT. Comparison to natural systems indicated that the critical shear strength of P1A in particular was quite high, while STP was similar to both river and wave-dominated freshwater environments (Droppo et al., 2007; Stone et al., 2008). Preliminary molecular analysis indicated microbial community variation indicative of the variation in age of each FFT product. P1A FFT contained a diversified and facultative community structure, while the microbial community within STP was more juvenile in nature.

4.2 Limitations and Future Work

The results obtained from this thesis research have given insight into similarities and differences between aged tailings FFT, from a biogeochemical framework to a dynamic shear based approach identifying material strength and erodibility characteristics. Throughout the study, although important results and conclusions have been made, there is always ways in which to improve upon future work, after identifying areas perhaps lacking in experimental design. In terms of the biogeochemical characterization explain in Chapter 2 of this thesis, improvement of headspace gas sampling could give even more accurate and precise means by which to measure the CH₄ release, and perhaps even detect H₂S in the headspace as well. Furthermore, identifying mineralogical changes within the FFT at specified depths

over time could give greater detail into the mineralogical changes caused by the biogeochemical alteration processes. With respect to the dynamic study explained in Chapter 3, there are also a few procedures that can be improved upon for future studies. First, it was determined that increased sample volume would have greatly increased the ability to extract useable quantities of DNA from the eroded FFT, and therefore, will be employed during the next round of experimentation. Furthermore, observation of filtered samples at various applied shear stresses will give increased spatial resolution with respect to particle characteristics and distribution at the FFT-OSPW interface and beyond.

Overall, these experimental improvements learned throughout the course of this thesis research can and will greatly improve upon future work utilizing similar FFT materials.

4.3 References

- Chen, M., Walshe, G., Chi Fru, E., Ciborowski, J.H., Weisener, C.G. 2013. Microcosm assessment of the biogeochemical development of sulfur and oxygen in oil sands fluid fine tailings. *App. Geochem.*, 37, 1 – 11.
- Droppo, I.G., Ross, N., Skafel, M., Liss, S.N. 2007. Biostabilization of cohesive sediment beds in a freshwater wave-dominated environment. *Limnol. Oceanogr.*, 52(2). 577 – 589.
- Holowenko, F.M., MacKinnon, M.D., Fedorak, P.M., 2000. Methanogens and sulphate-reducing bacteria in oil sands fine tailings waste. *Can J Microbiol.*, 46(10), 927 – 937.
- Stone, M., Krishnappan, B.G., Emelko, M.B. 2008. The effect of bed age and shear stress on the particle morphology of eroded cohesive river sediment in an annular flume. *Water Research*, 42, 4179 – 4187.
- [In Preparation] VanMensel et al., 2015 – The Proteobacteria response and genomic features of gamma-irradiated oil sands fluid fine tailings: a community structure perspective.
- Voordouw, G. 2013. Interaction of oil sands tailings particles with polymers and microbial cells: First steps toward reclamation to soil. *Biopolymers*, 99(4), 257 – 262.

APPENDIX A (*Co-author letters of permission*)

Chapter 2 Permissions



University
of Windsor

Thomas Reid <reid11c@uwindsor.ca>

Re: Declaration of Co-authorship For Thesis

6 messages

Thomas Reid <reid11c@uwindsor.ca> Fri, Jan 23, 2015 at 8:54 PM

To: Ryan Boudens <boudens@uwindsor.ca>, Danielle Vanmensen
<vanmensd@uwindsor.ca>, Sabari Mullapulli Raveendran
<mullapus@uwindsor.ca>, Chris Weisener <weisener@uwindsor.ca>, Jan
Ciborowski <cibor@uwindsor.ca>

Hello co-authors,

Part of my MSc thesis paper includes data and results that will be published in the following paper:

Title:

"Physicochemical gradients, diffusive flux, and sediment oxygen demand within oil sands tailings material from Alberta, Canada"

Authors:

T. Reid; R. Boudens; D. VanMensen; S. Prakasan M.R.; J. Ciborowski; C. Weisener

Status:

In prep for submission

I am requesting from each of you, permission to use these results and findings in my thesis as part of my Ch.2, as you are the co-authors on the above publication. Please make it clear in a simple email response that you (be sure to include your name in the response) give me permission (or not) as it must be included in my submitted thesis in the appendix.

If you have any questions let me know...

Thanks so much,
Thomas Reid

Danielle Vanmensen <vanmensd@uwindsor.ca>
To: Thomas Reid <reid11c@uwindsor.ca>

Fri, Jan 23, 2015 at 11:21 PM

Hi Tom,

You absolutely have my permission to use these results and findings in your thesis.

Thanks for asking!

Danielle VanMensen
[Quoted text hidden]

Christopher Weisener <weisener@uwindsor.ca>

Sat, Jan 24, 2015 at 9:03 AM

To: Thomas Reid <reid11c@uwindsor.ca>
Cc: Ryan Boudens <boudens@uwindsor.ca>, Danielle Vanmensen <vanmensd@uwindsor.ca>, Sabari Mullapulli Raveendran <mullapus@uwindsor.ca>, Ciborowski Jan <cibor@uwindsor.ca>

you have my permission

Dr. Christopher Weisener
Associate Professor
Geomicrobiology/Geochemistry
Coordinator Biomaterials Laboratory
GLIER/EES Department
University Of Windsor
401 Sunset Ave. Windsor ,ON
N9B3P4

[Quoted text hidden]

Sabari Mullapulli Raveendran <mullapus@uwindsor.ca>

Sat, Jan 24, 2015 at 9:16 AM

To: Thomas Reid <reid11c@uwindsor.ca>
Cc: Ryan Boudens <boudens@uwindsor.ca>, Danielle Vanmensen <vanmensd@uwindsor.ca>, Chris Weisener <weisener@uwindsor.ca>, Jan Ciborowski <cibor@uwindsor.ca>

Dear Thomas Reid

You have my permission

Thanks

Sabari Prakasan M.R

[Quoted text hidden]

Jan Ciborowski <cibor@uwindsor.ca>

Sat, Jan 24, 2015 at 2:19
PM

To: mullapus@uwingmail.uwindsor.ca

Cc: reid11c@uwingmail.uwindsor.ca, boudens@uwingmail.uwindsor.ca,
vanmensd@uwingmail.uwindsor.ca, Chris Weisener <weisener@uwindsor.ca>

... and my permission, too.

Cheers, Jan

Jan J.H. Ciborowski
Dept. of Biological Sciences
University of Windsor
Windsor, ON,
CANADA, N9B 3P4

Tel.: [\(519\) 253-3000 ext. 2725](tel:(519)253-3000)
Fax: [\(519\) 971-3609](tel:(519)971-3609)
e-mail: cibor@uwindsor.ca

CoChair, Lake Erie Millennium Network. Visit the web page
at: <http://www.LEMN.org>
Biological Sciences web page: <http://www.uwindsor.ca/biology>

-----Sabari Mullapulli Raveendran <mullapus@uwindsor.ca>
wrote: -----

To: Thomas Reid <reid11c@uwindsor.ca>

From: Sabari Mullapulli Raveendran <mullapus@uwindsor.ca>

Date: 01/24/2015 09:16AM

Cc: Ryan Boudens <boudens@uwindsor.ca>, Danielle Vanmensen
<vanmensd@uwindsor.ca>, Chris Weisener
<weisener@uwindsor.ca>, Jan Ciborowski <cibor@uwindsor.ca>

Subject: Re: Declaration of Co-authorship For Thesis

[Quoted text hidden]

Ryan Boudens <boudens@uwindsor.ca>

Sun, Jan 25, 2015 at 9:31 PM

To: Thomas Reid <reid11c@uwindsor.ca>

Cc: Danielle Vanmensen <vanmensd@uwindsor.ca>, Sabari Mullapulli Raveendran <mullapus@uwindsor.ca>, Chris Weisener <weisener@uwindsor.ca>, Jan Ciborowski <cibor@uwindsor.ca>

You have permission to publish as co-author for the thesis mentioned above.

Ryan Boudens

On Fri, Jan 23, 2015 at 8:54 PM, Thomas Reid <reid11c@uwindsor.ca> wrote:

[Quoted text hidden]

Chapter 3 Permissions:



University
of Windsor

Thomas Reid <reid11c@uwindsor.ca>

Re: Declaration of Co-authorship Ch.3

3 messages

Thomas Reid <reid11c@uwindsor.ca>

Sun, Jan 25, 2015 at 10:14 AM

To: "Droppo,Ian [Burlington]" <Ian.Droppo@ec.gc.ca>, Chris Weisener <weisener@uwindsor.ca>

Hello Chris and Ian,

Part of my MSc thesis paper includes data and results that will be published in the following paper:

Title (Tentative):

"Critical Shear Strength and Biostabilization of industrial tailings materials"

Authors:

T. Reid; I. Droppo, C. Weisener

Status:

In prep for submission

I am requesting from each of you, permission to use these results and findings in my thesis as part of my Ch.3, as you are the co-authors on the above publication. Please make it clear in a simple email response that you (be sure to include your name in the response) give me permission (or not) as I must include these emails in the appendix of my thesis.

If you have any questions let me know...

Thanks so much,
Thomas Reid

Droppo,Ian [Burlington] <Ian.Droppo@ec.gc.ca> Sun, Jan 25, 2015 at 2:59 PM
To: reid11c@uwindsor.ca

Permission granted.
Ian

From: Thomas Reid [mailto:reid11c@uwindsor.ca]
Sent: Sunday, January 25, 2015 10:14 AM
To: Droppo,Ian [Burlington]; Chris Weisener <weisener@uwindsor.ca>
Subject: Re: Declaration of Co-authorship Ch.3

[Quoted text hidden]

Christopher Weisener <weisener@uwindsor.ca> Sun, Jan 25, 2015 at 4:33 PM
To: Thomas Reid <reid11c@uwindsor.ca>
Cc: "Droppo,Ian [Burlington]" <Ian.Droppo@ec.gc.ca>

You have my permission

Cheers

Dr. Christopher Weisener
Associate Professor
Geomicrobiology/Geochemistry
Coordinator Biomaterials Laboratory
GLIER/EES Department
University Of Windsor
401 Sunset Ave. Windsor ,ON
N9B3P4

VITA AUCTORIS

NAME:	Thomas C. Reid
PLACE OF BIRTH:	Barrie, Ontario, Canada
YEAR OF BIRTH:	1989
EDUCATION:	University of Western Ontario, (H)B.Sc Geophysics, London, ON, Canada 2011 University of Windsor, M.Sc Environmental Science, Windsor, ON, Canada 2015